COMBUSTION RESEARCH FACILITY

SAND2014-3118P

Progress Towards In-Cylinder PIV Measurements throughout the Full Intake and Compression Strokes

Kan Zha, Stephen Busch, Paul Miles
Sandia National Laboratories

Unclassified, Unlimited Release

Sandia National Laboratories is a multi-program laboratory managed and operated by Sandia Corporation, a wholly owned subsidiary of Lockheed Martin Corporation, for the U.S. Department of Energy's National Nuclear Security Administration under contract DE-AC04-94AL85000

Motivation

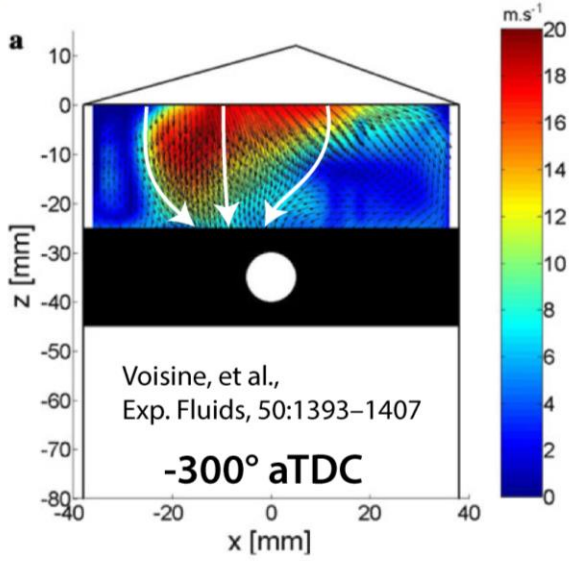

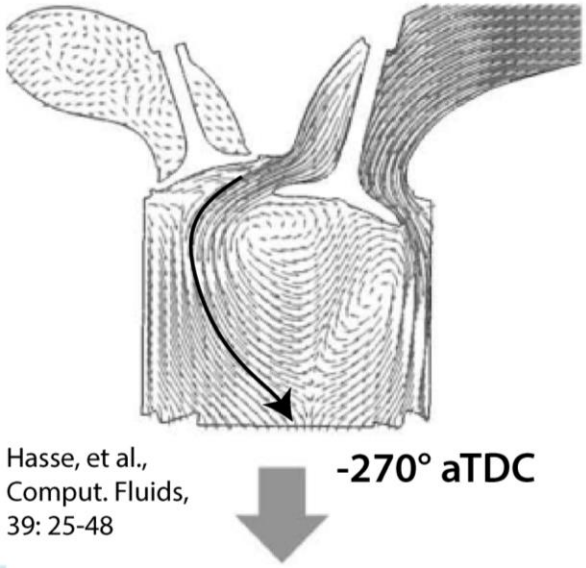

- Why use piston with conventional bowl geometry?
  - In-cylinder flow characterized by valve jets-piston top interactions in the first part of induction stroke.
  - Cyclic variability influenced by jet-piston interactions (identified by experiments and hybrid RANS-LES modeling).
  - Bowl-in-piston cylinder geometries can substantially change the in-cylinder flow.

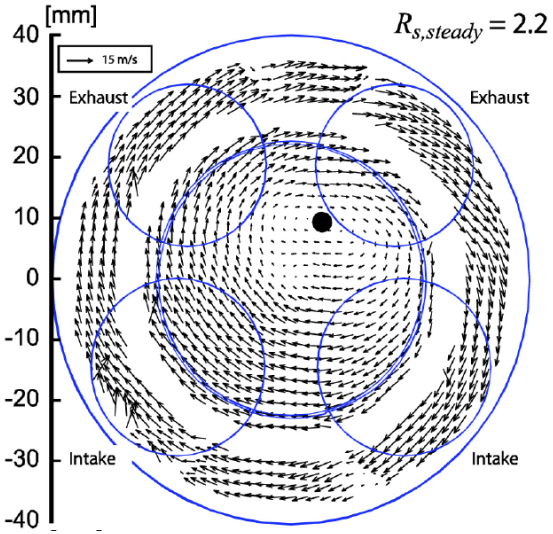

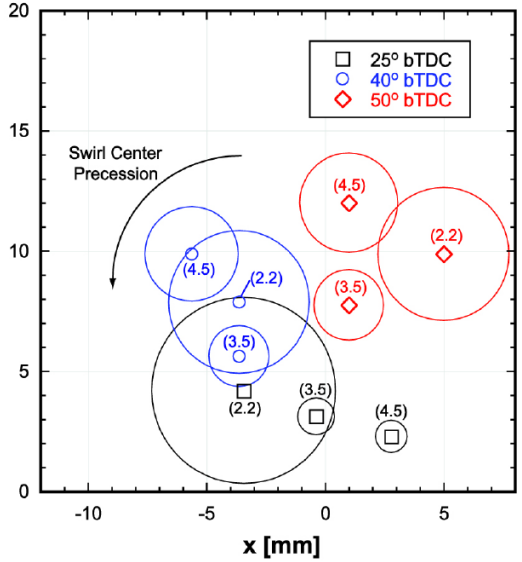

Petersen, SAE2011-01-1285

Experimental setup and swirl-plane measurement test cases

GM 1.9 L Diesel Engine	
Bore	82 mm
Stroke	90.4 mm
Displacement Volume	0.477 L
Geometries CR	16.7
Squish Height	0.78 mm
Intake / Exhaust Valves	2 / 2
Swirl Ratio	1.5, 2.2, 3.5
Engine Speed	1500 rpm
Intake Pressure	1.5 bar
Intake Temperature	99 degC
Coolant Temperature	~89 degC
O2 Mole Fraction	10%

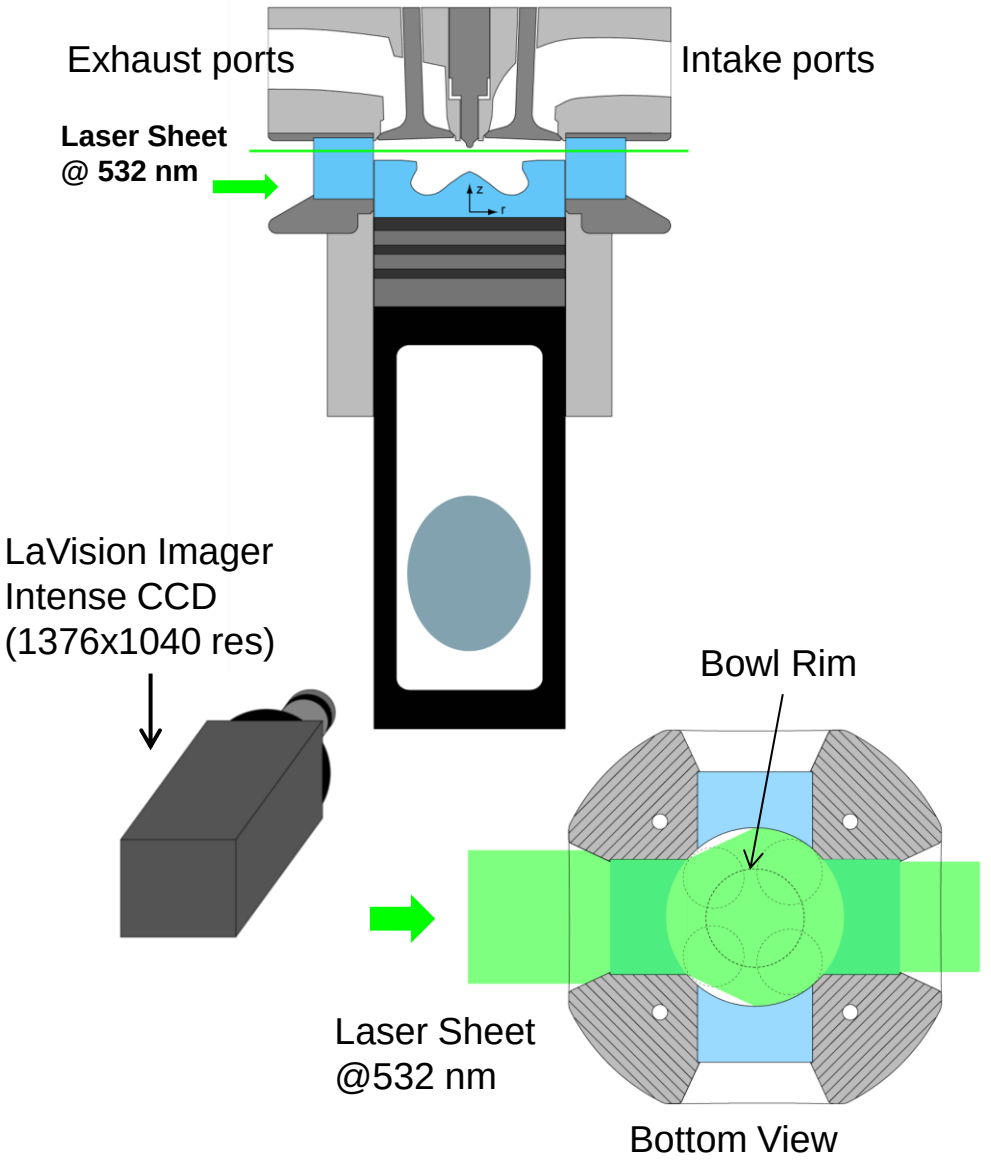

Swirl-plane measurement test cases

- Swirl planes are chosen to minimize laser scattering by intake valves and piston
- Laser sheet minimum waist diameter around 2 mm
  - Consistent with 32 x 32 interrogation region (~2 mm x 2mm)
  - Mainly considering out-of-plane motion during intake stroke
- Every 15 CAD throughout intake and compression stroke (green region)

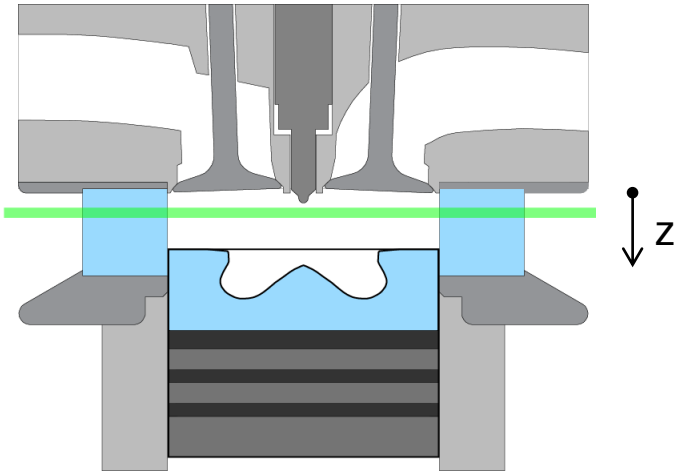

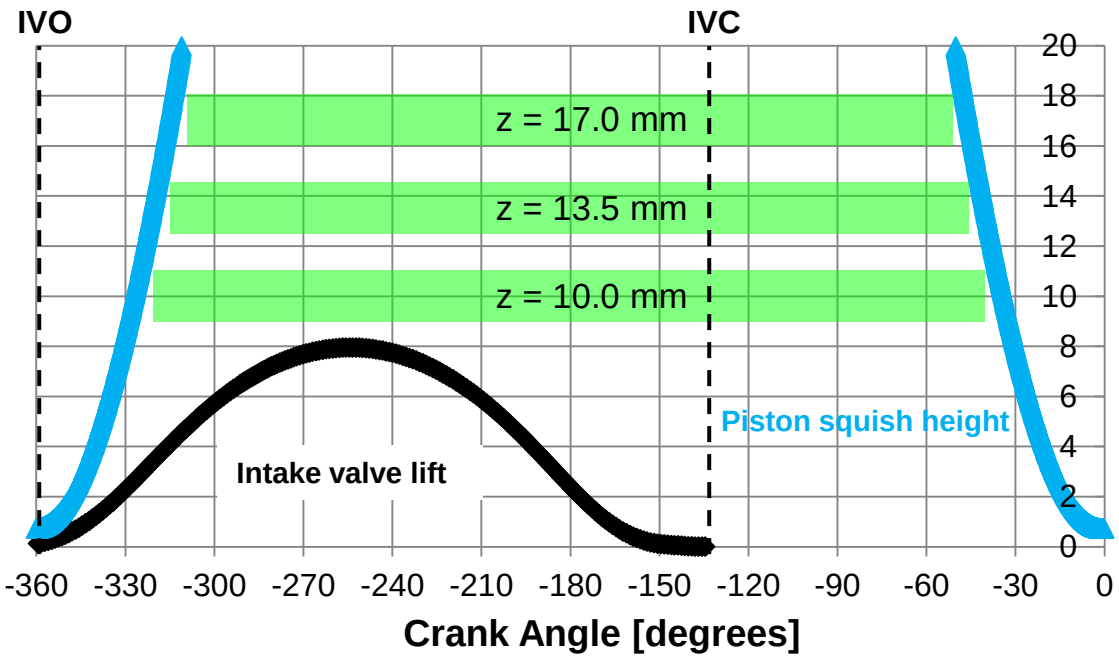

PIV tracer selection

Aerosol → size ~= 1 µm, Mie-scattering signal is too weak through piston

Borosilicate glass

- 2 µm, little lag error, but induces ring torque problem
- 18 µm, lag error during early intake, and ring torque problem

Lycopodium → size =32 µm, good ring torque, but induces large lag error

Both timescale calculation (from Converge simulation) and PIV results showed that 2µm borosilicate glass would follow more flow structures during intake stroke.

Lycopodium (32 µm)

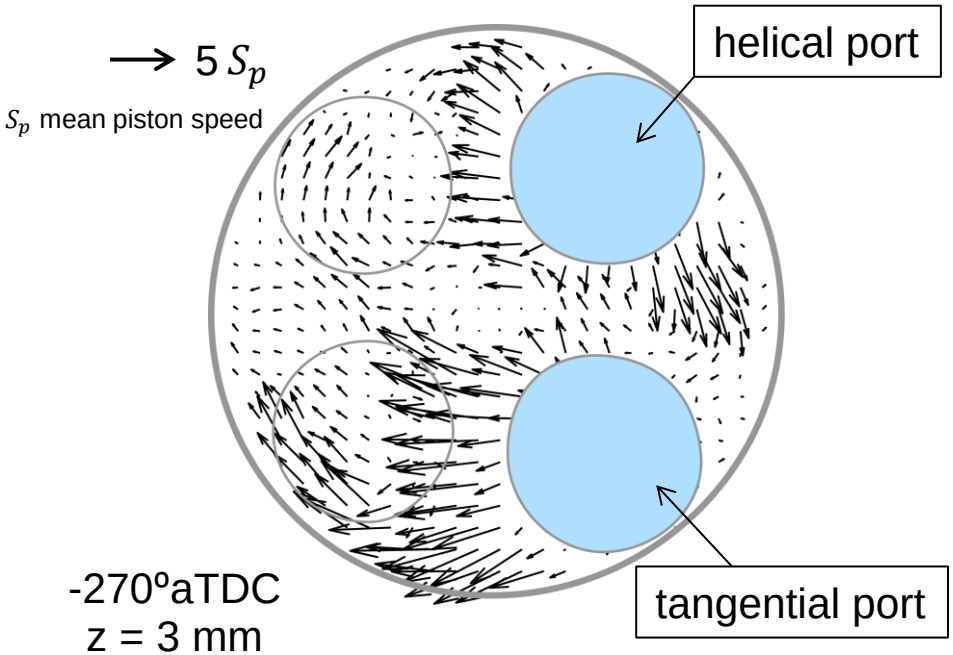

Borosilicate glass (2 µm)

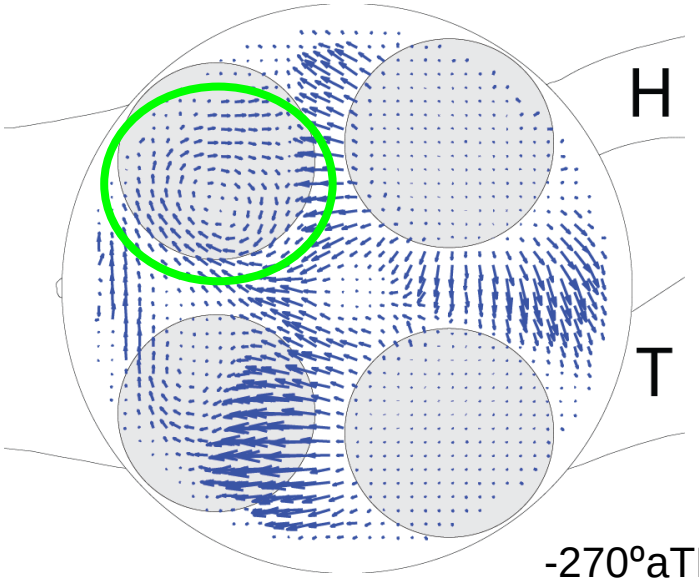

Conventional bowl geometries induce significant uncertainties due to image degradation and severe distortion

- Image degradation is more severe when piston close to BDC
- Distortion is dependent on pixel radius location and piston position
- Distortion pattern is different in bowl, squish zone and valve cut-out region

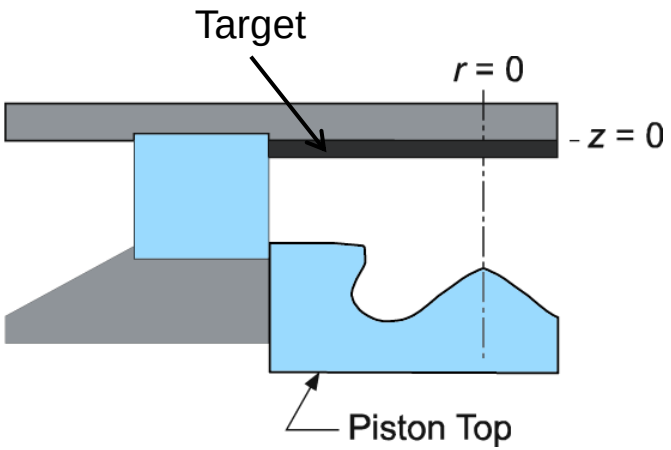

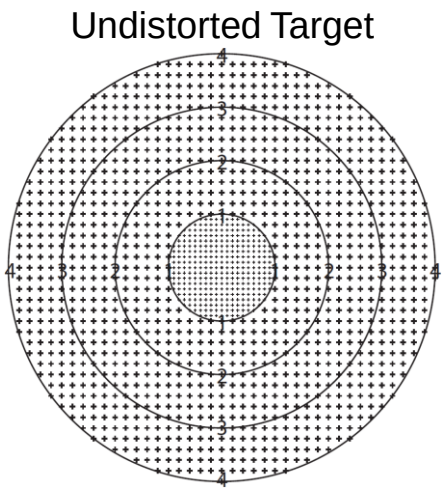

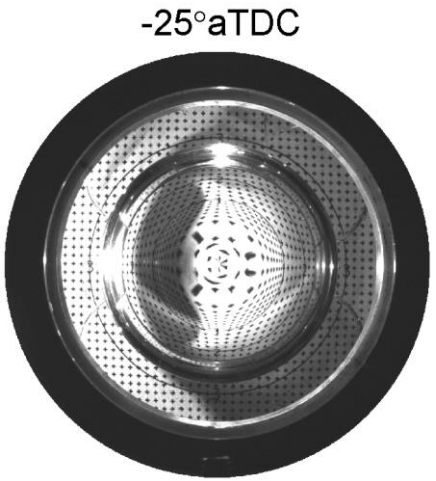

Conventional bowl geometries induce significant uncertainties due to highly distorted image

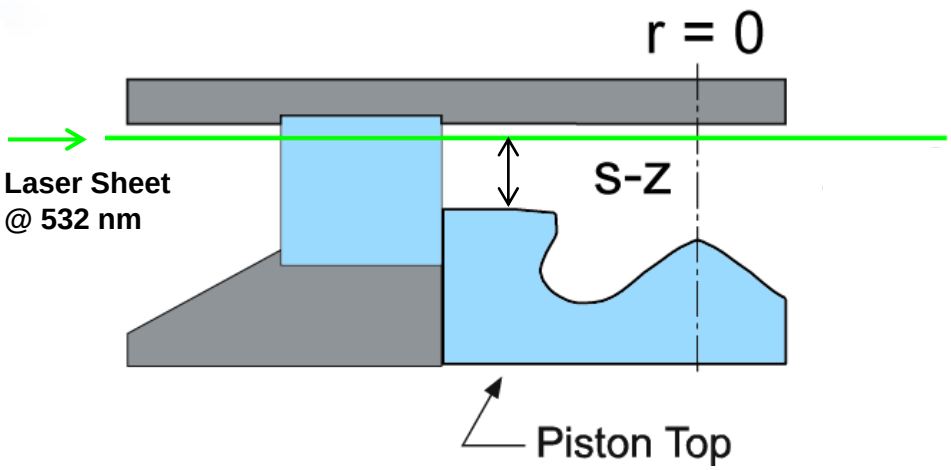

Raw Mie-Scattering Images

-90◦aTDC

- Distortion is dependent on piston motion (instantaneous speed and position) during Δt (time interval between two laser pulses).
  - Higher image resolution (61μm/pixel) is desired for better accuracy, but longer Δt is required for particle displacement to match ~¼ of interrogation window size (minimum 32x32 pixels).
  - Different Δt is needed for different dynamic range of velocities during compression and intake strokes.

Conventional bowl geometries induce significant uncertainties due to highly distorted image

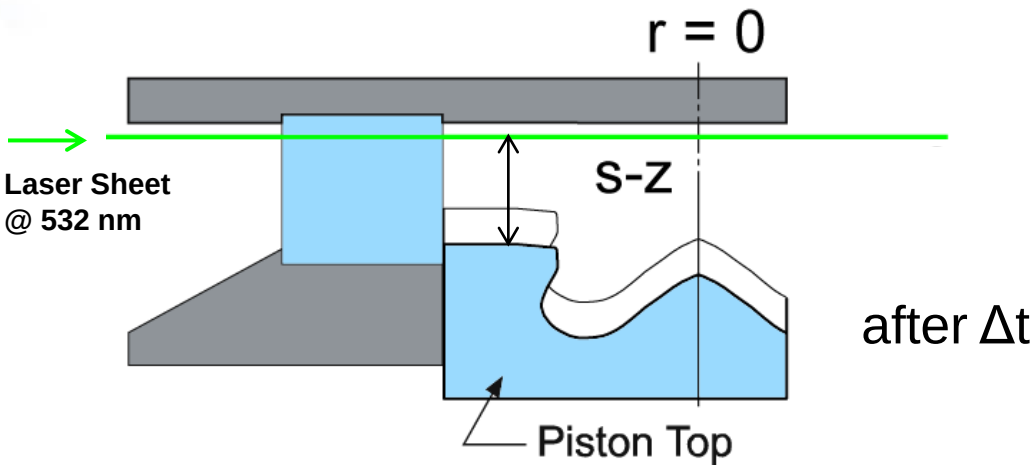

- Piston position (s) changes

→ Image becomes bigger / smaller (at fixed s-z), local distortion changes.

- Distance between measurement plane to piston (s-z) changes

→ Distortion pattern changes.

- Distortion is dependent on piston motion (instantaneous speed and position) during Δt (time interval between two laser pulses).
  - Higher image resolution (61μm/pixel) is desired for better accuracy, but longer Δt is required for particle displacement to match ~¼ of interrogation window size (minimum 32x32 pixels).
  - Different Δt is needed for different dynamic range of velocities during compression and intake strokes.

General mapping procedure

- Step One: R → r’

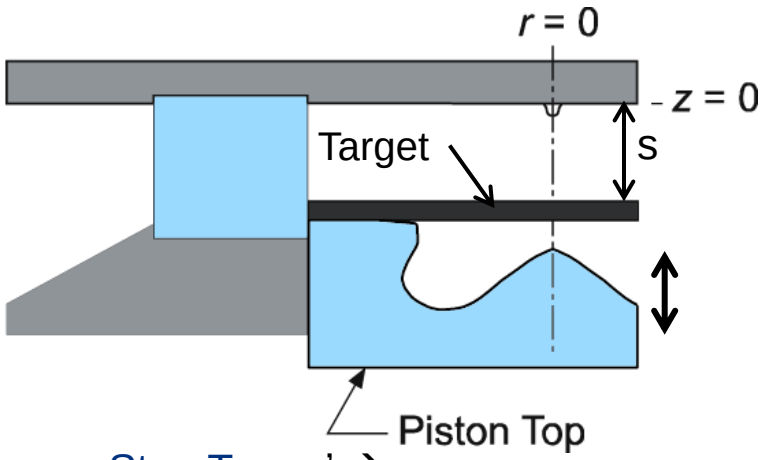

- Step Two: r’ → r

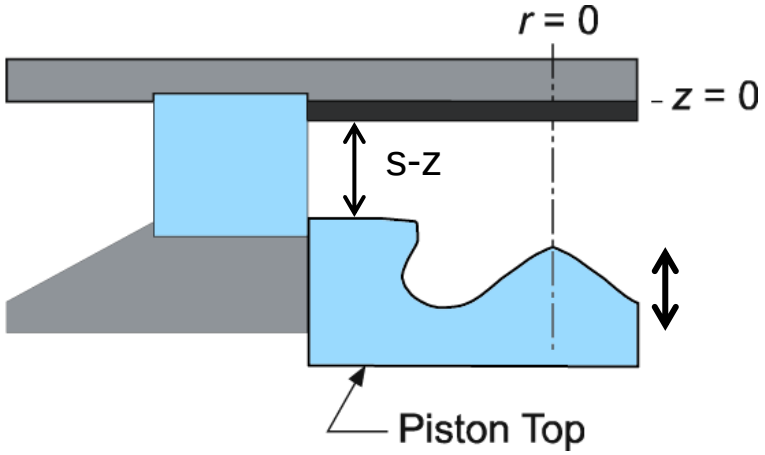

Raw Target Image

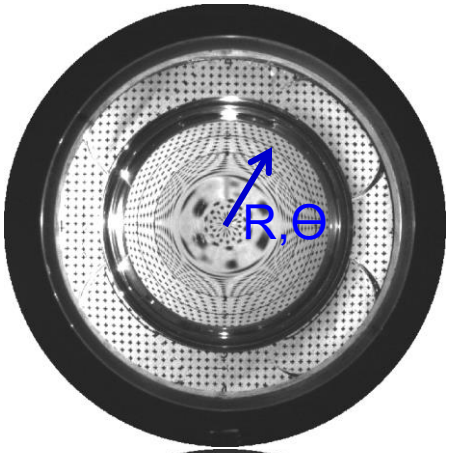

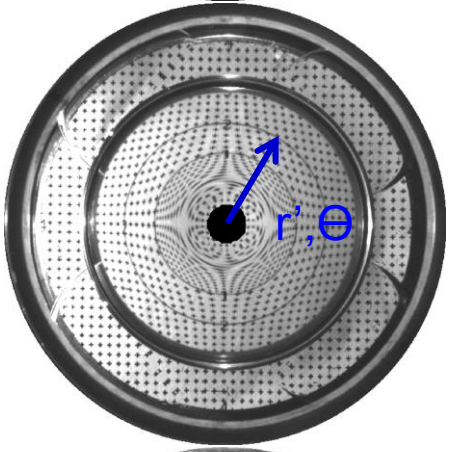

Physical Space

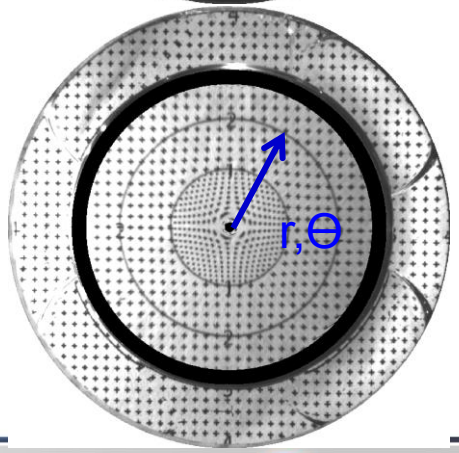

General mapping procedure

- Step One: R → r’

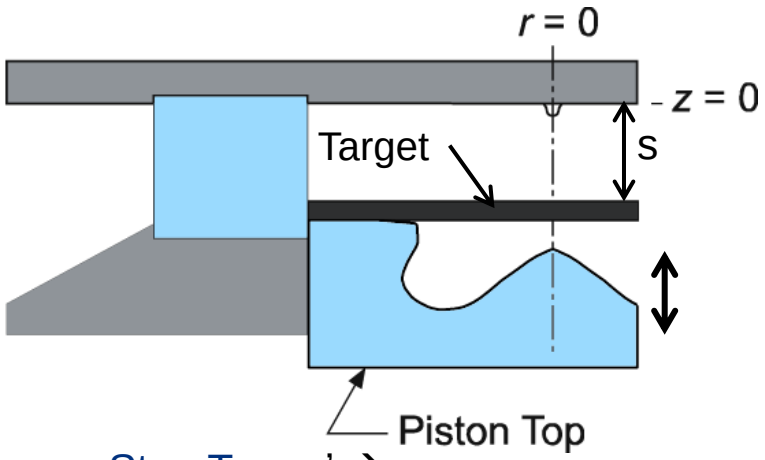

- Step Two: r’ → r

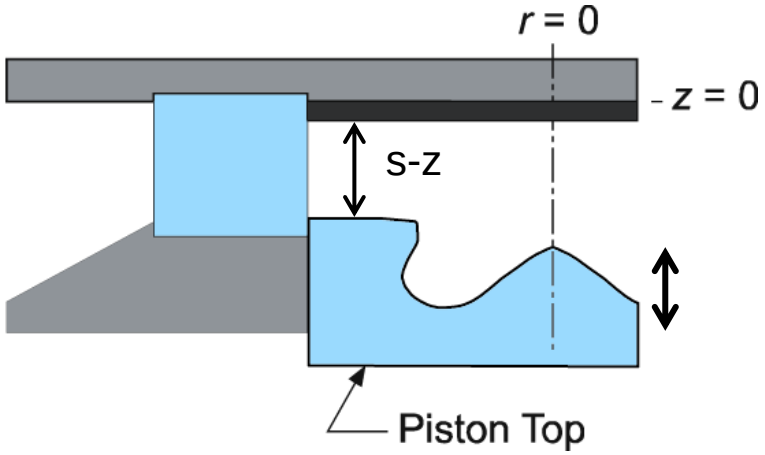

- Map X → x
  X: locations in a highly distorted image
  x: physical space
- Due to the axisymmetric bowl, portions of the distorted image corresponding to parts of target image viewed through the bowl can be mapped in terms of a radial coordinate R → r
- Mapping R → r’ accounts for magnification and local distortion effects with changes of s.

$$r' = r_0' + k_1(s - s_0)$$

$$k_1 = aR^3 + bR^2 + cR + d$$

- Mapping r’ → r accounts for distortion effects with changes of s-z.

$$r = R_0 + k_2(r' - R_0')$$

$$k_2 = \alpha(s - z)^2 + \beta(s - z) + \gamma$$

- Combining the two mappings:

$$r = R_0 + k_2\left[r_0' + k_1(s - s_0) - R_0'\right]$$

R_0, R_0', r_0', s_0 are constants known from calibration.

General mapping procedure

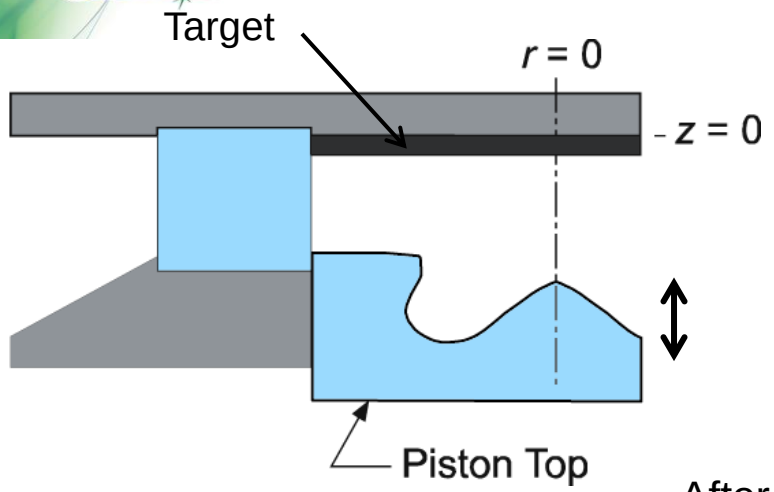

- Difficult to map marks near the injector tip (r<5 mm) due to severe distortion.
- Local no-solution areas near injector exist in some dewarped images.

Raw Target Frame

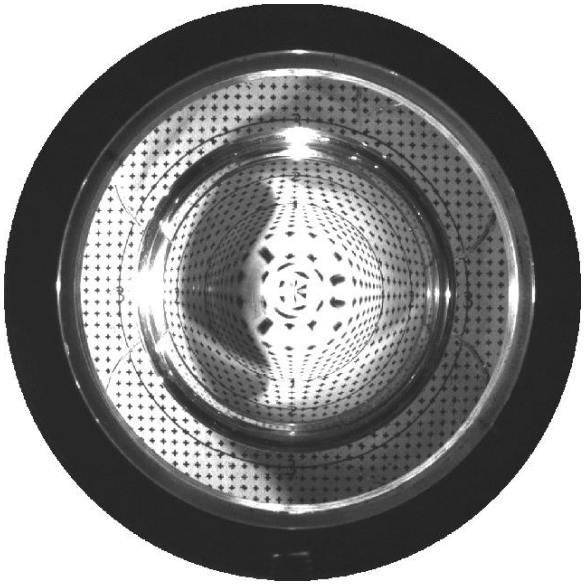

After magnification and local distortion correction

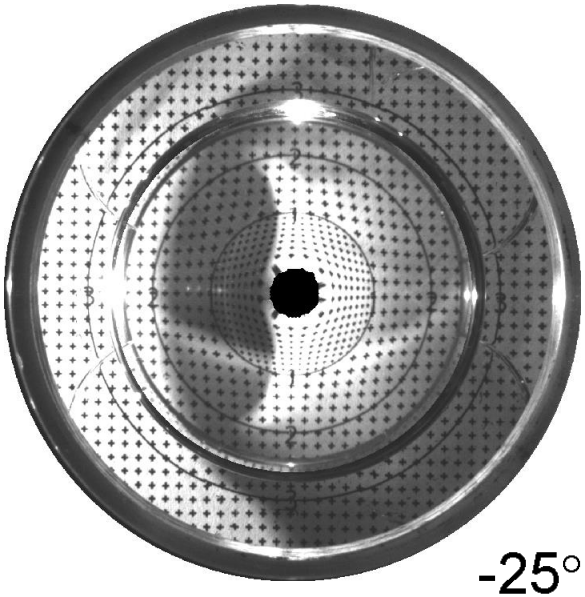

After distortion correction (final dewarping result)

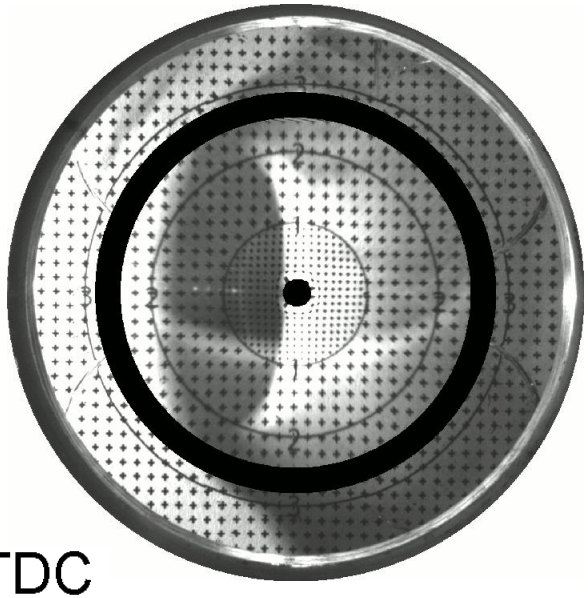

-25°aTDC

PIV pre-processing and dewarping

Velocity Field Processing	
Preprocessing	Laser energy fluctuation correction
	Laser spatial fluence
	Seed density change
	Background subtraction
	Dewarping with “general mapping procedure”

Velocity Field Processing	
Preprocessing	N/A
Vector calculation	Cross-correlation: standard I1*I2 (via FFT, no zero-padding), iterative multi-pass.
	Minimum interrogation window size, 32x32 pixels, 50% overlap
Multi-pass postprocessing	Delete vector if peak ratio Q<1.3 Median filter: strongly remove and iterative replace: remove if diff. to avg. > 2*r.m.s. of neighbours (re)insert if diff. to avg. < 3*r.m.s. of neighbours Remove groups with <5 vectors
Vector postprocessing	Allowable vector range (0 ~ 60 m/s) Median filter

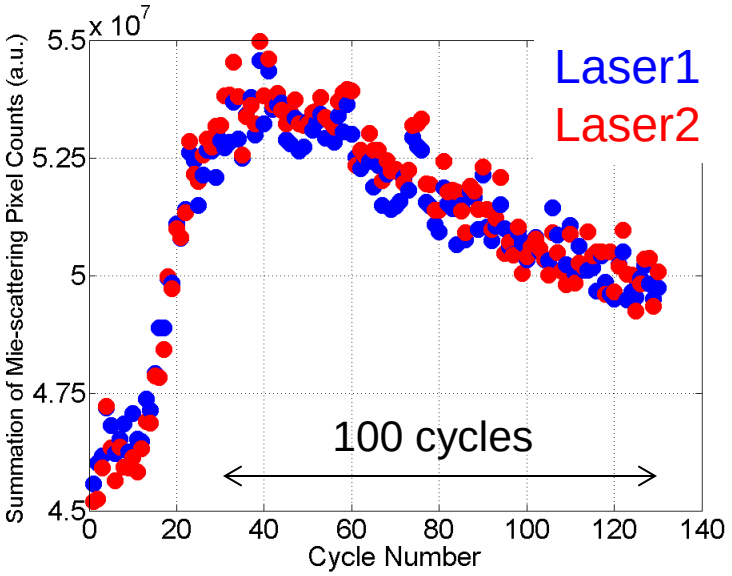

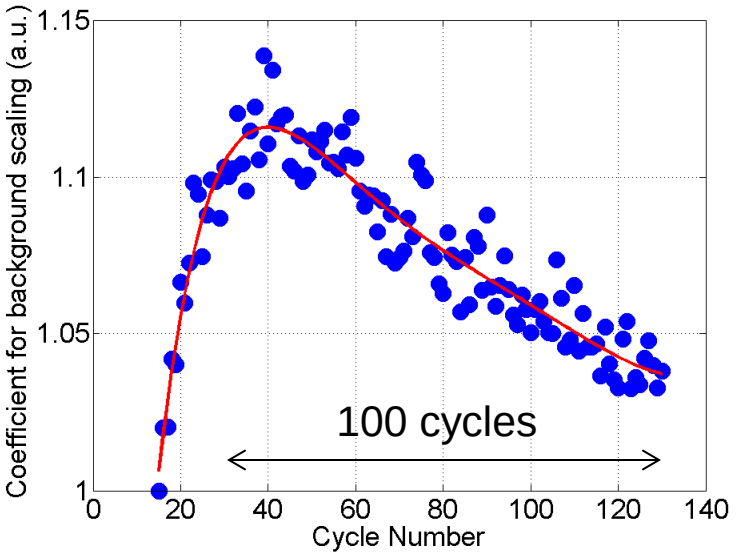

GM swirl ratio index, z=10mm

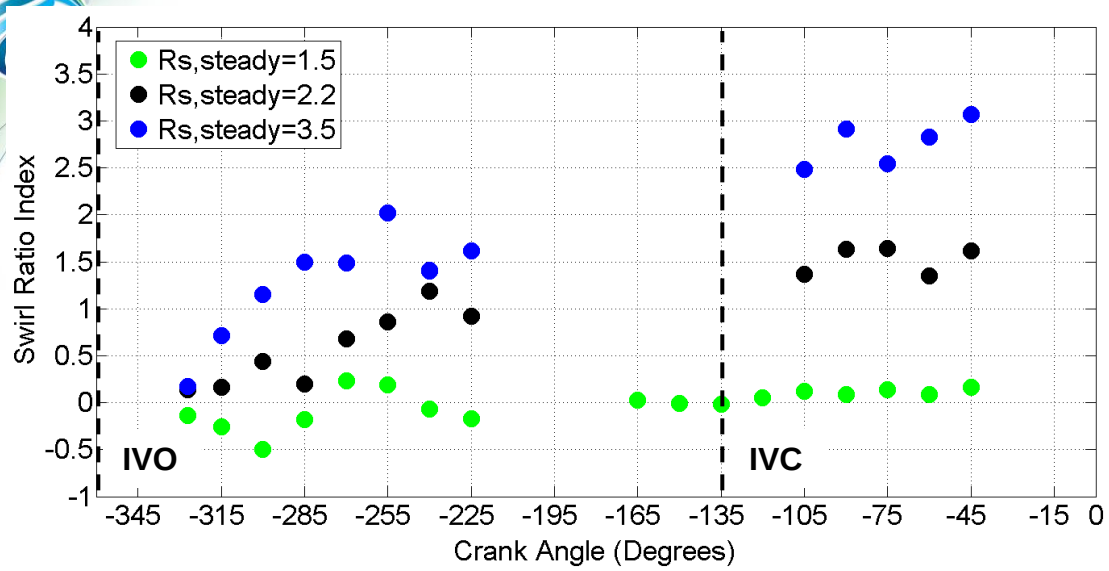

- Complex flow structures observed during intake stroke
- Little swirl is observed at Rs,steady=1.5
- Spurious vectors mainly generated by laser background scattering, signal-to-noise is worse close to BDC

Rs,steady=1.5

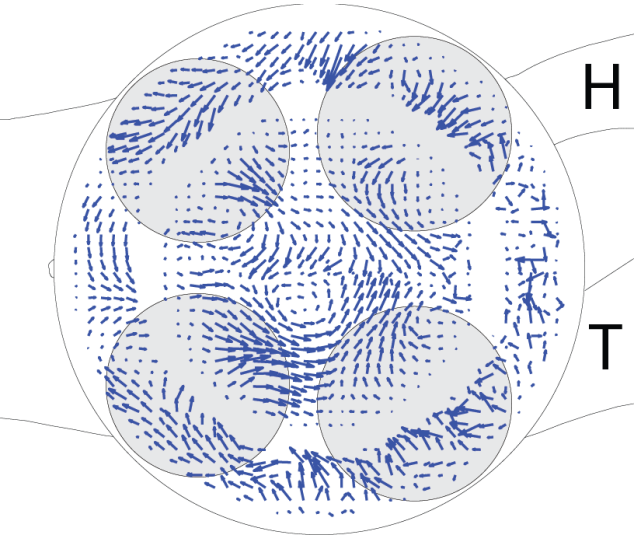

Rs,steady=2.2

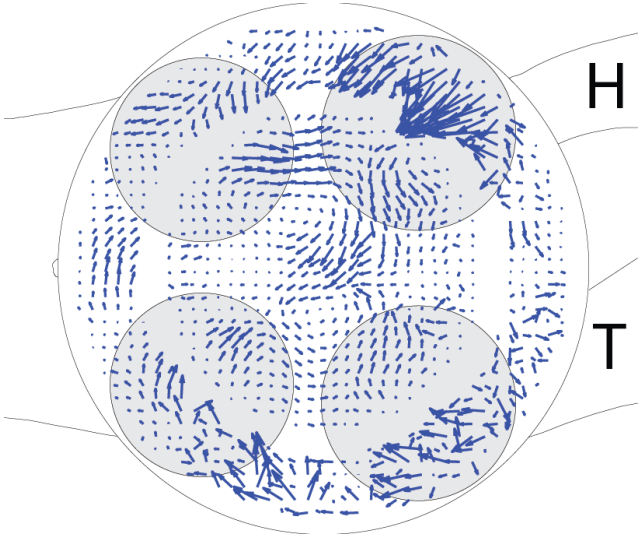

Rs,steady=3.5

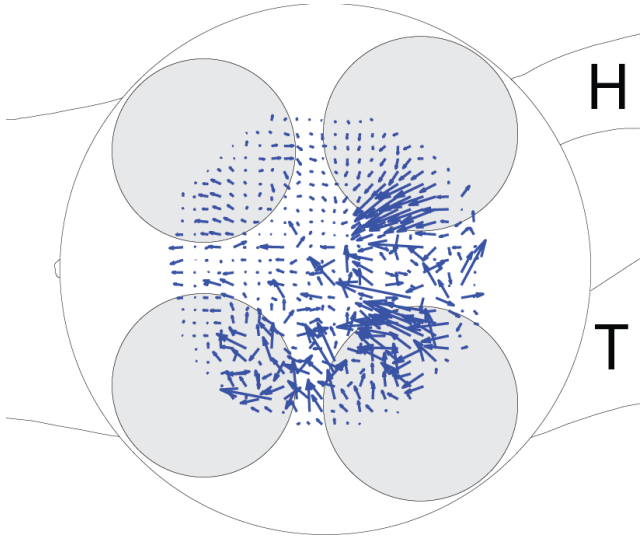

Ensemble mean-velocity over 100 cycles

-327°aTDC

→ 5 S_p

GM swirl ratio index, z=10mm

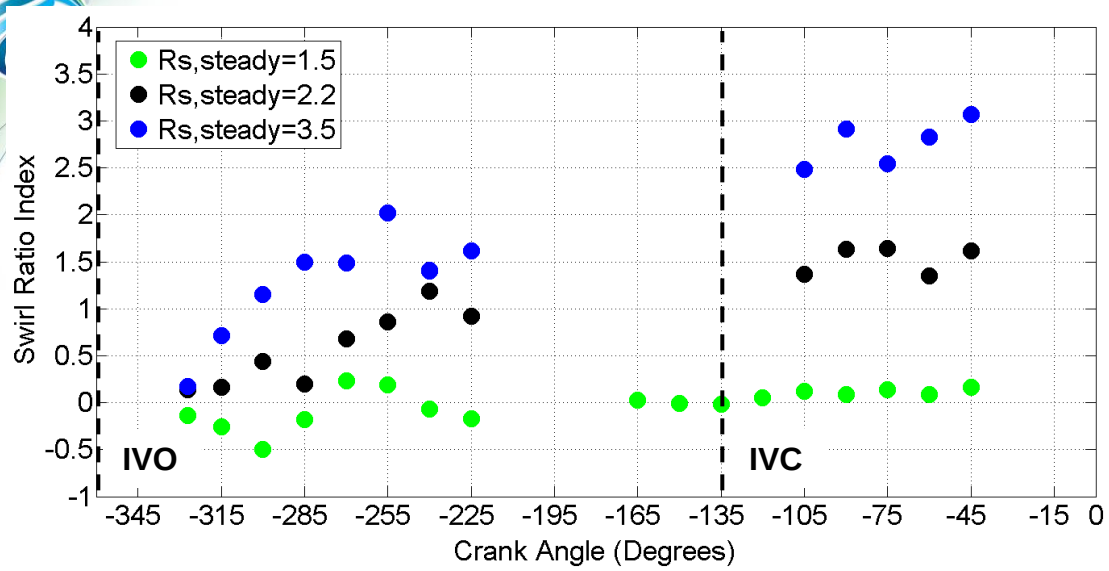

- Complex flow structures observed during intake stroke
- Little swirl is observed at Rs,steady=1.5
- Spurious vectors mainly generated by laser background scattering, signal-to-noise is worse close to BDC

Rs,steady=1.5

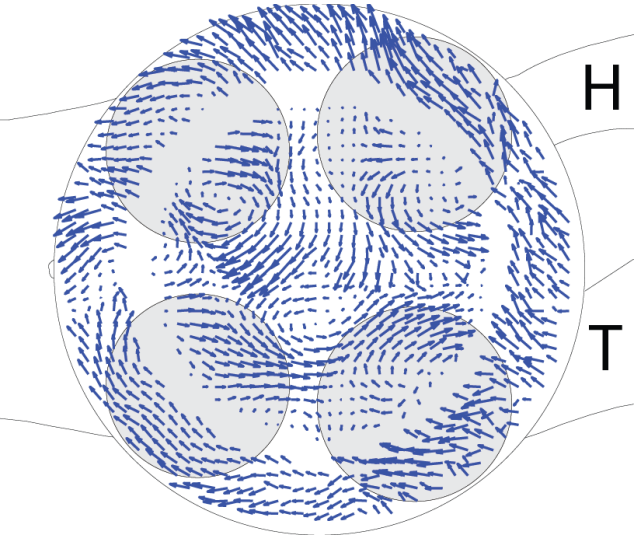

Rs,steady=2.2

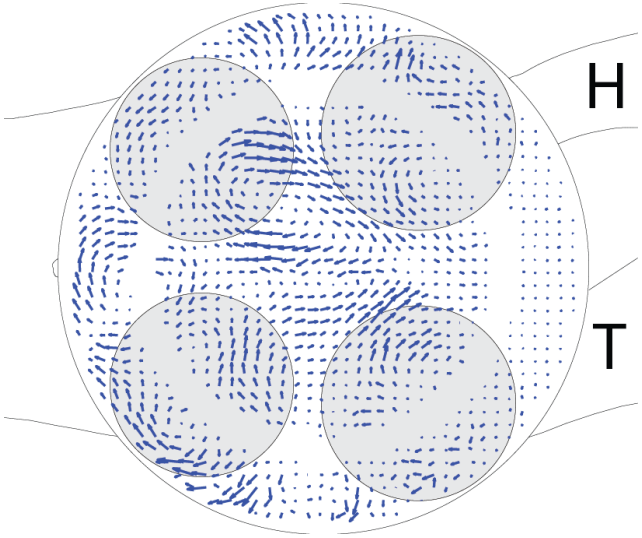

Rs,steady=3.5

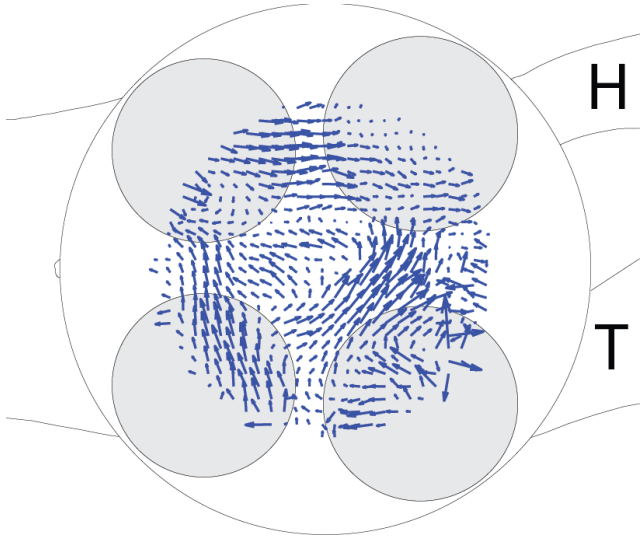

Ensemble mean-velocity over 100 cycles

-315°aTDC

→ 5 S_p

GM swirl ratio index, z=10mm

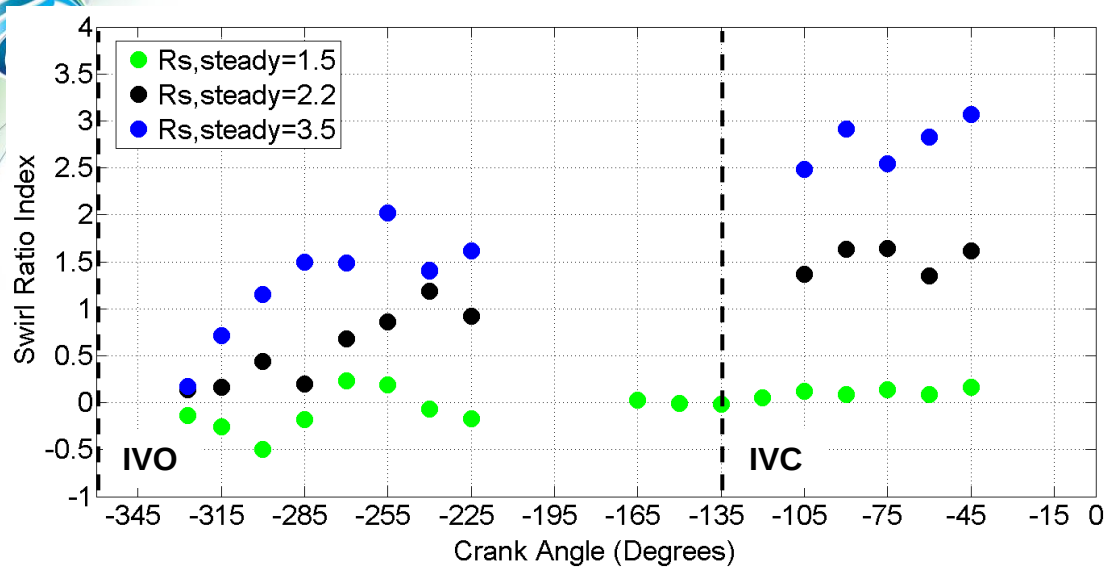

- Complex flow structures observed during intake stroke
- Little swirl is observed at Rs,steady=1.5
- Spurious vectors mainly generated by laser background scattering, signal-to-noise is worse close to BDC

Rs,steady=1.5

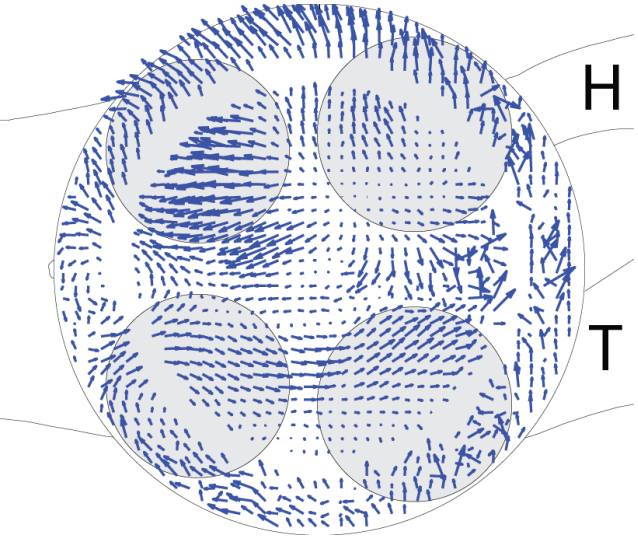

Rs,steady=2.2

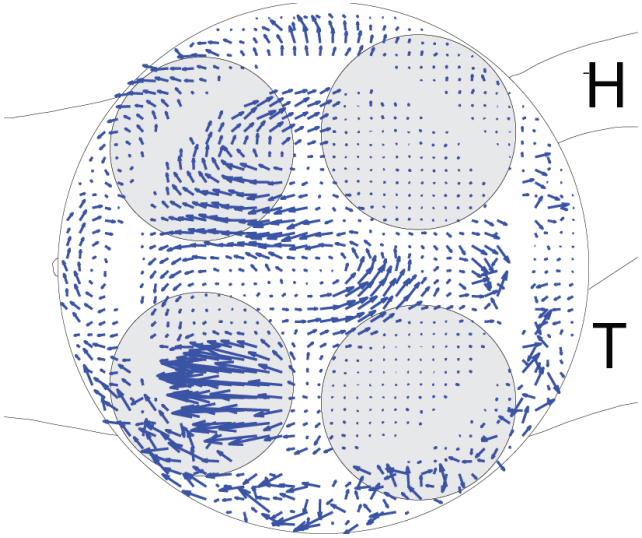

Rs,steady=3.5

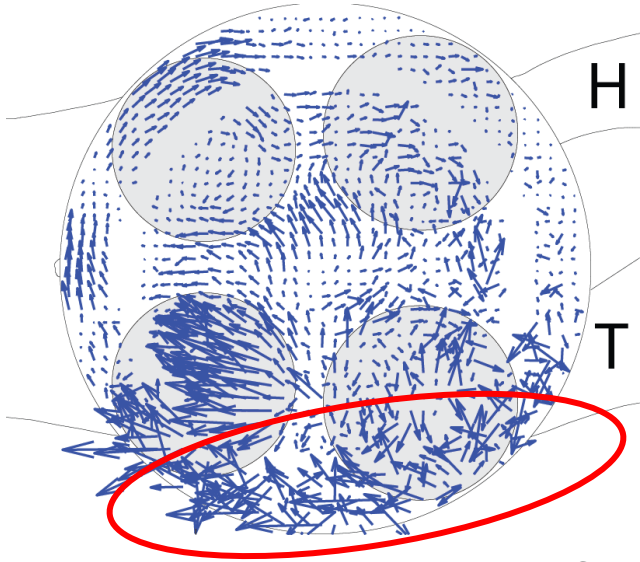

Ensemble mean-velocity over 100 cycles

-300°aTDC

→ 5 S_p

GM swirl ratio index, z=10mm

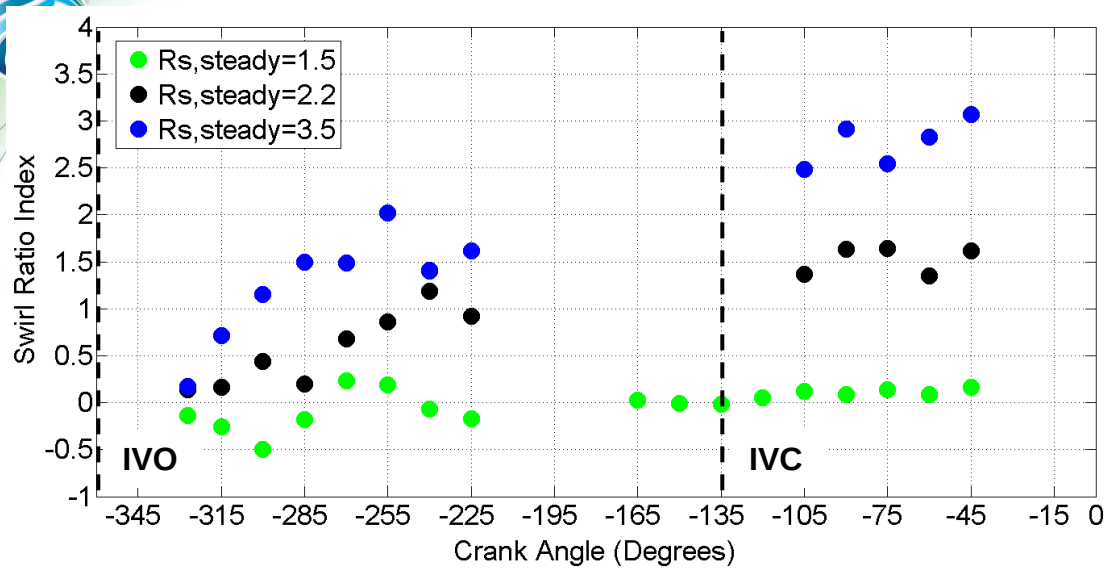

- Complex flow structures observed during intake stroke
- Little swirl is observed at Rs,steady=1.5
- Spurious vectors mainly generated by laser background scattering, signal-to-noise is worse close to BDC

Rs,steady=1.5

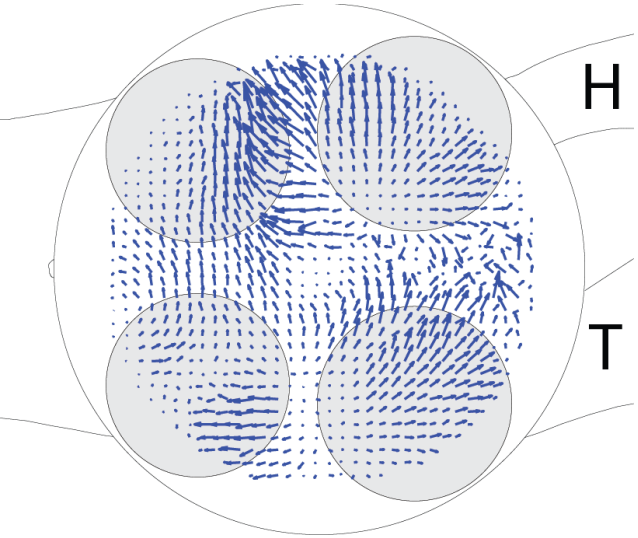

Rs,steady=2.2

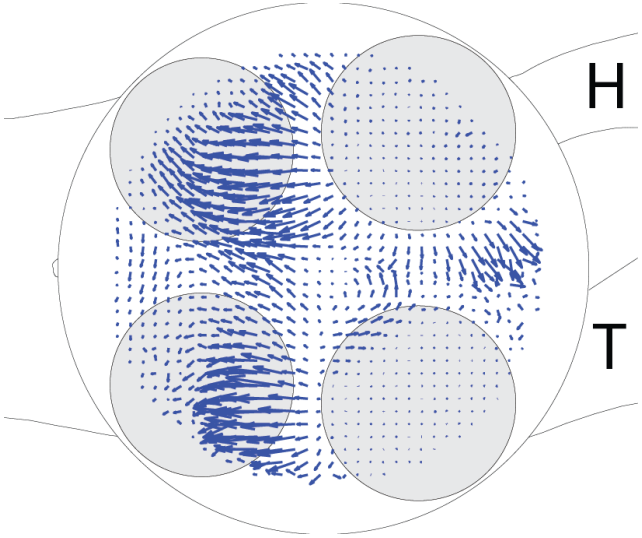

Rs,steady=3.5

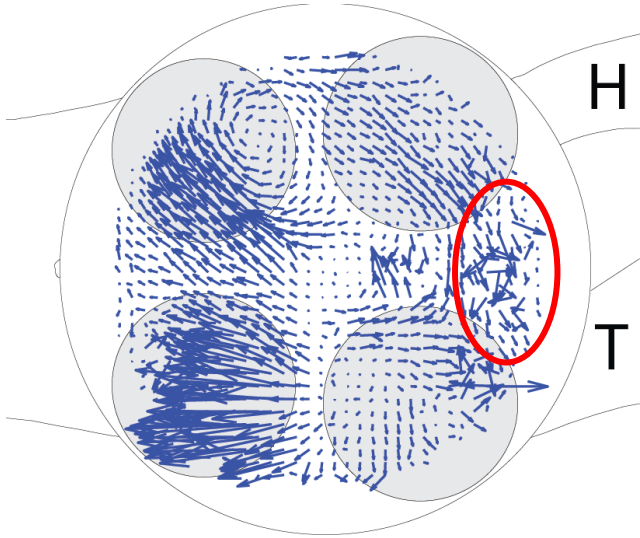

Ensemble mean-velocity over 100 cycles

-285°aTDC

→ 5 S_p

GM swirl ratio index, z=10mm

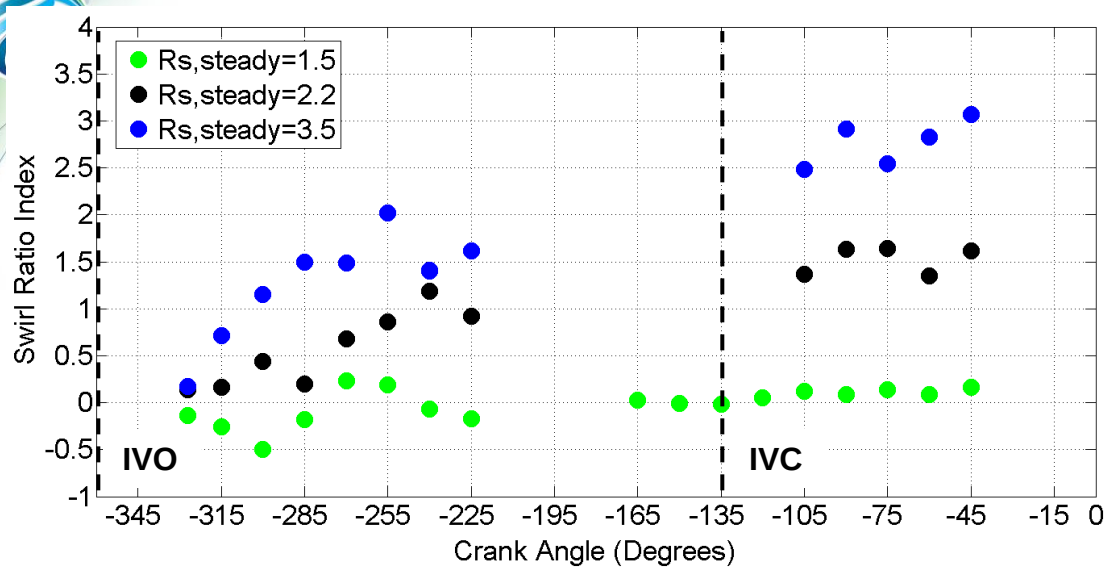

- Complex flow structures observed during intake stroke
- Little swirl is observed at Rs,steady=1.5
- Spurious vectors mainly generated by laser background scattering, signal-to-noise is worse close to BDC

Rs,steady=1.5

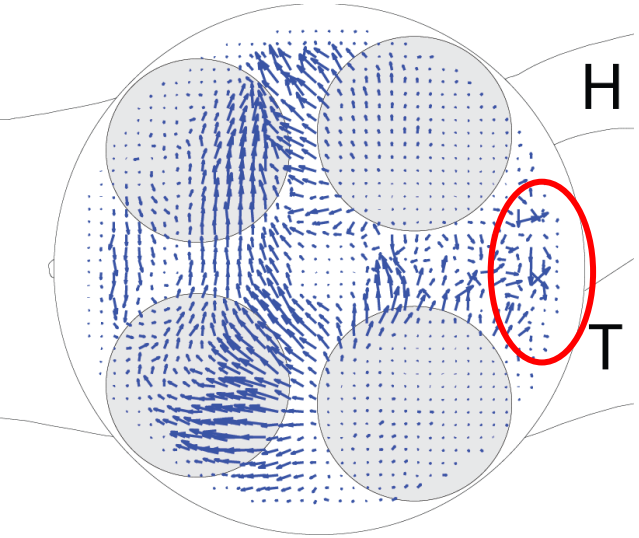

Rs,steady=2.2

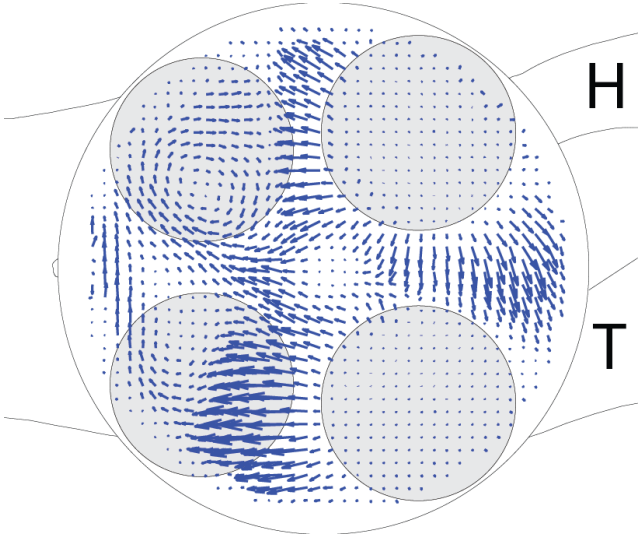

Rs,steady=3.5

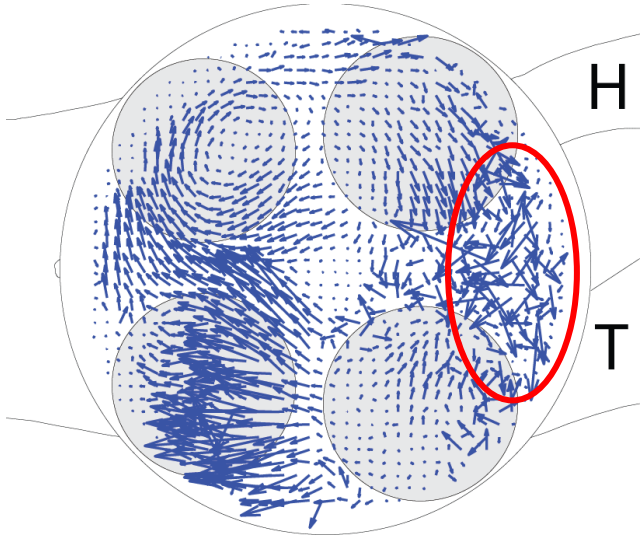

Ensemble mean-velocity over 100 cycles

-270°aTDC

→ 5 S_p

GM swirl ratio index, z=10mm

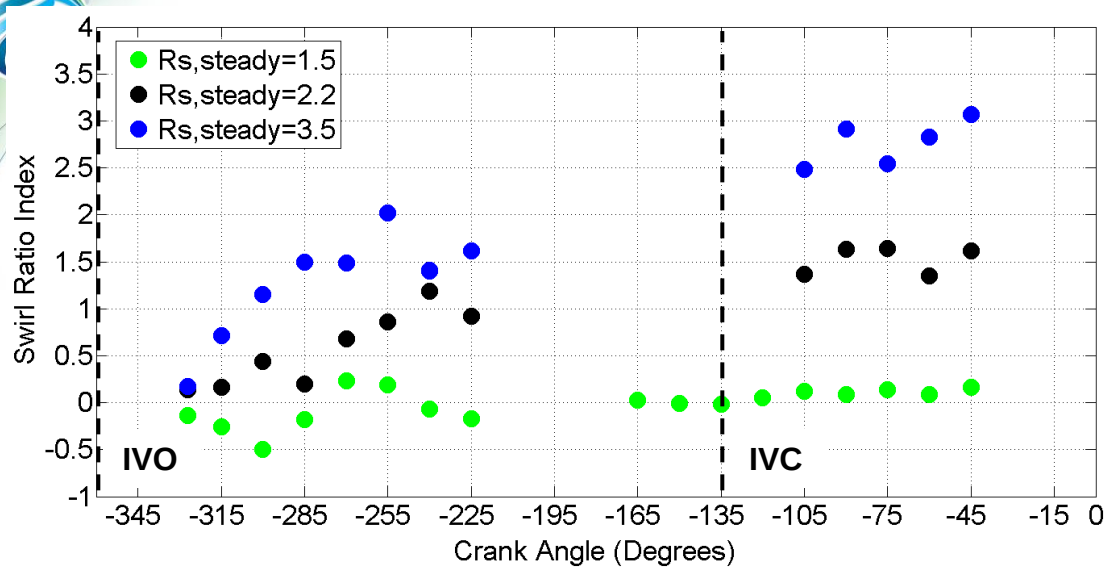

- Complex flow structures observed during intake stroke
- Little swirl is observed at Rs,steady=1.5
- Spurious vectors mainly generated by laser background scattering, signal-to-noise is worse close to BDC

Rs,steady=1.5

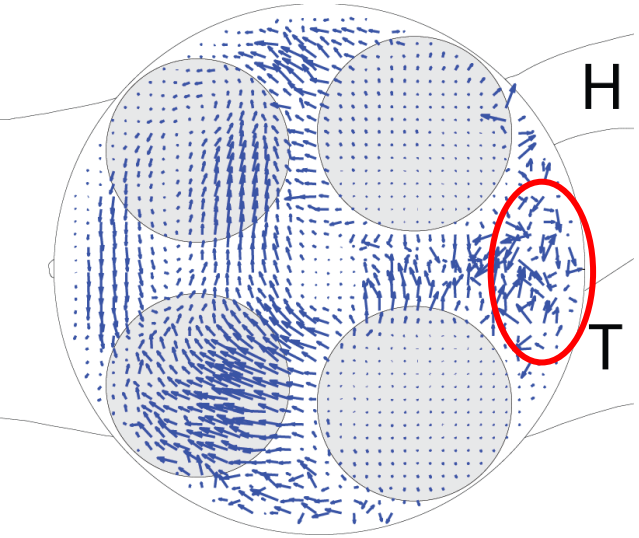

Rs,steady=2.2

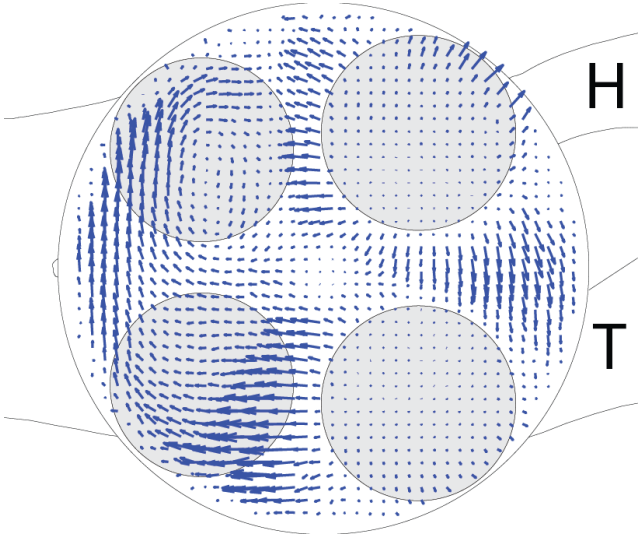

Rs,steady=3.5

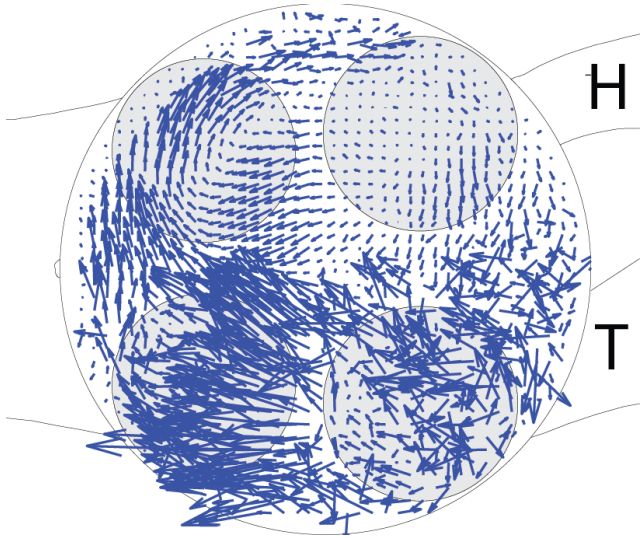

Ensemble mean-velocity over 100 cycles

-255°aTDC

→ 5 S_p

GM swirl ratio index, z=10mm

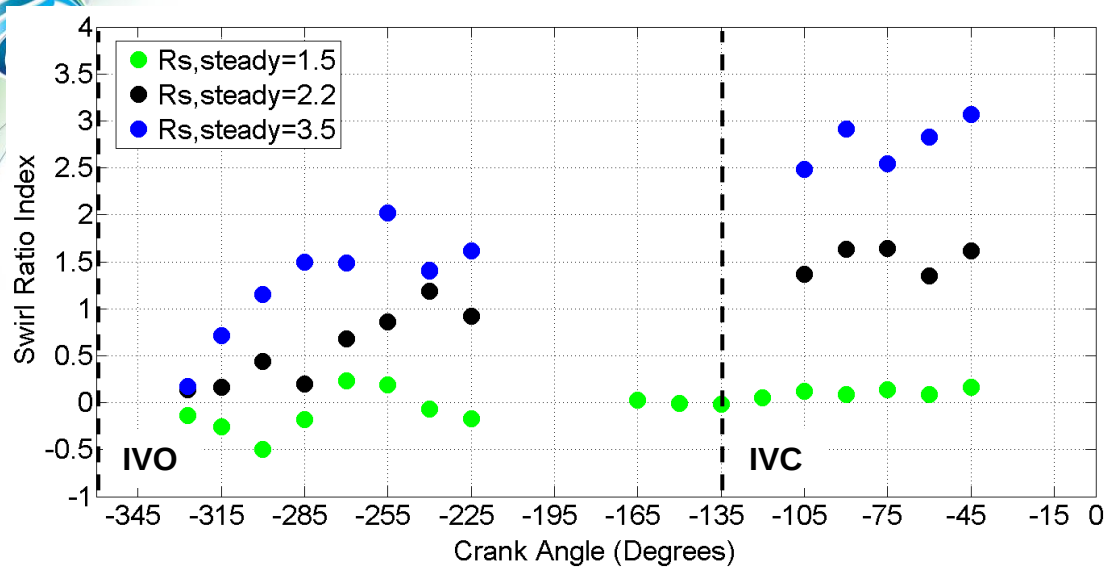

- Complex flow structures observed during intake stroke
- Little swirl is observed at Rs,steady=1.5
- Spurious vectors mainly generated by laser background scattering, signal-to-noise is worse close to BDC

Rs,steady=1.5

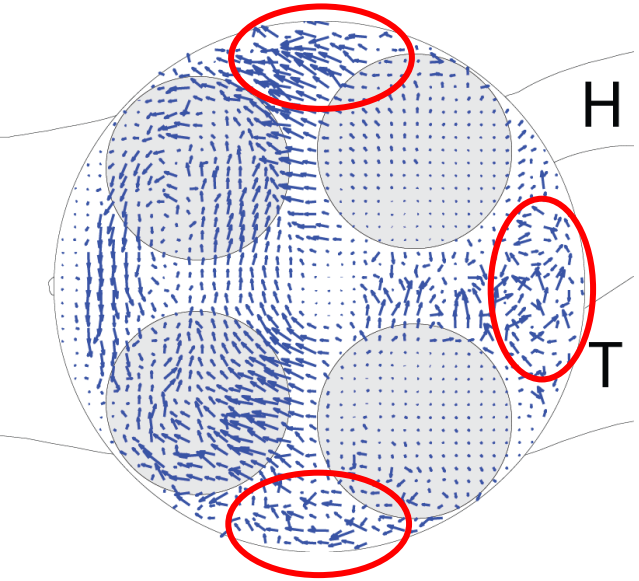

Rs,steady=2.2

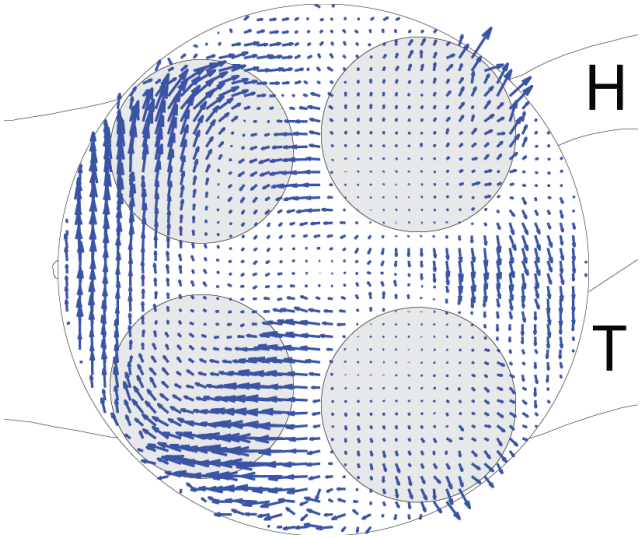

Rs,steady=3.5

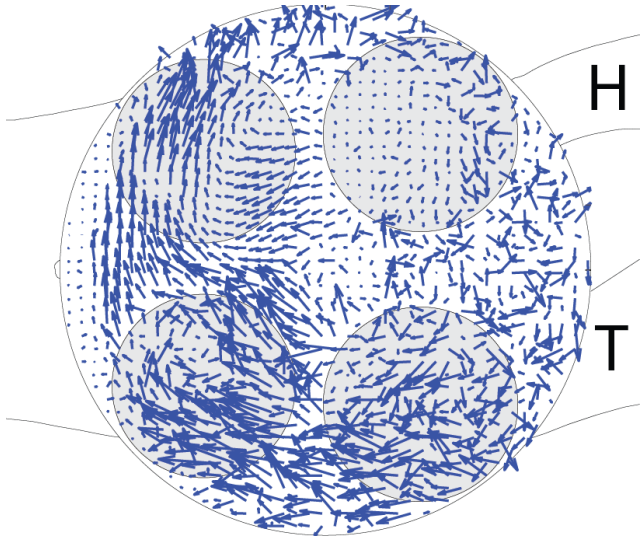

Ensemble mean-velocity over 100 cycles

-240°aTDC

$\longrightarrow 5\,S_p$

GM swirl ratio index, z=10mm

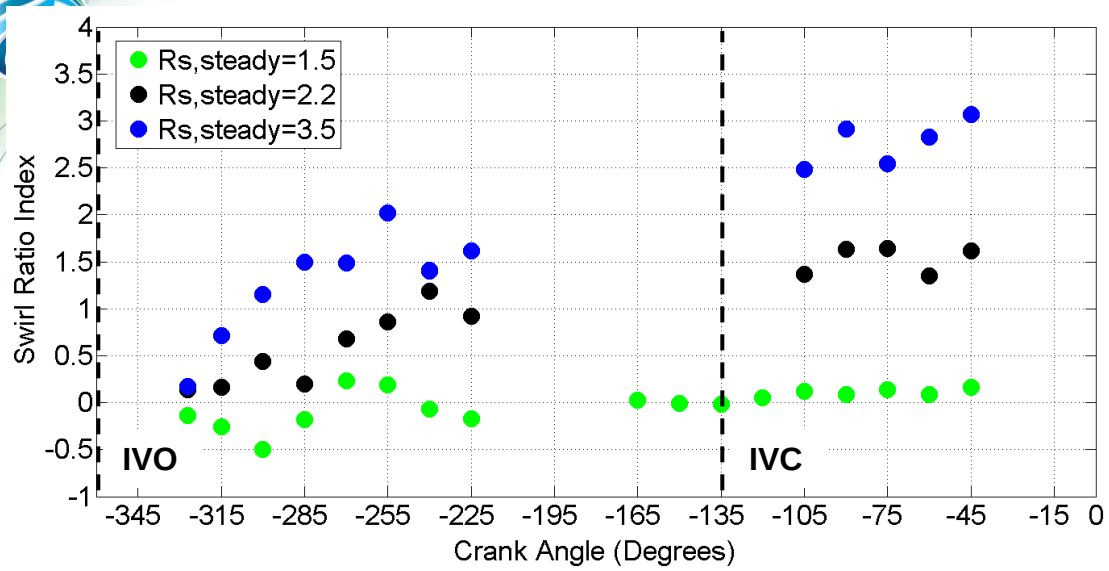

- Complex flow structures observed during intake stroke
- Little swirl is observed at Rs,steady=1.5
- Spurious vectors mainly generated by laser background scattering, signal-to-noise is worse close to BDC

Rs,steady=1.5

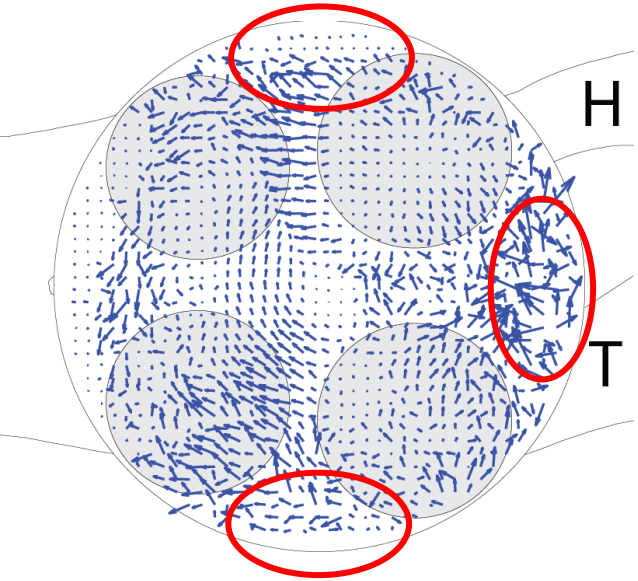

Rs,steady=2.2

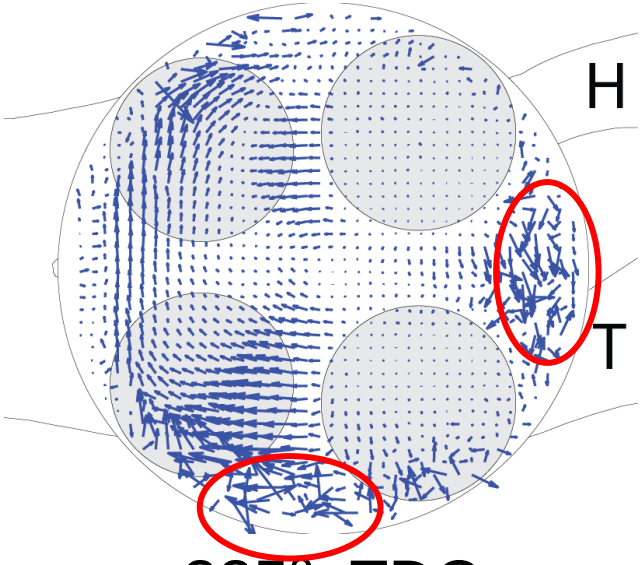

Rs,steady=3.5

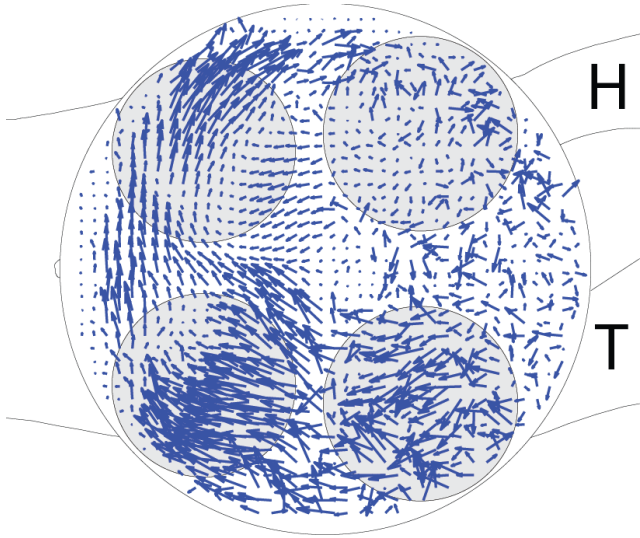

Ensemble mean-velocity over 100 cycles

-225ºaTDC

→ 5 S_p

GM swirl ratio index, z=10mm

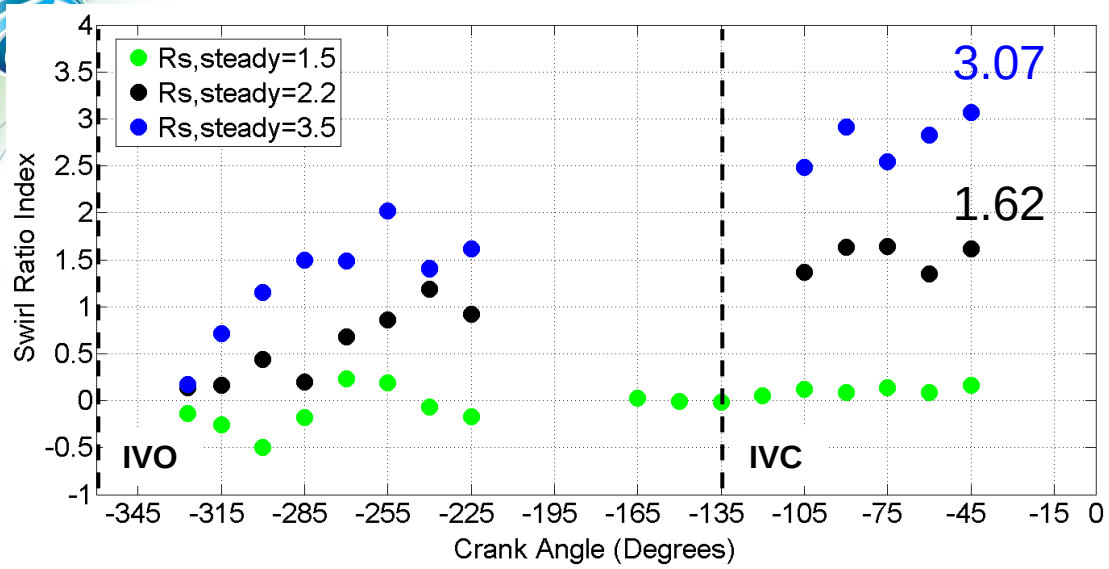

Swirl ratio index definition

$$\omega_z = \frac{\sum_{z=10mm} \left(xU_y - yU_x \right)}{\sum_{z=10mm} \left(x^2 + y^2 \right)}$$

$$R_s = \frac{\omega_z}{2\pi N}$$

x, y x,y coordinate of interrogation window center relative to chamber center (m)

U_x, U_y x,y velocity components from PIV (m/s)

Rs,steady=1.5

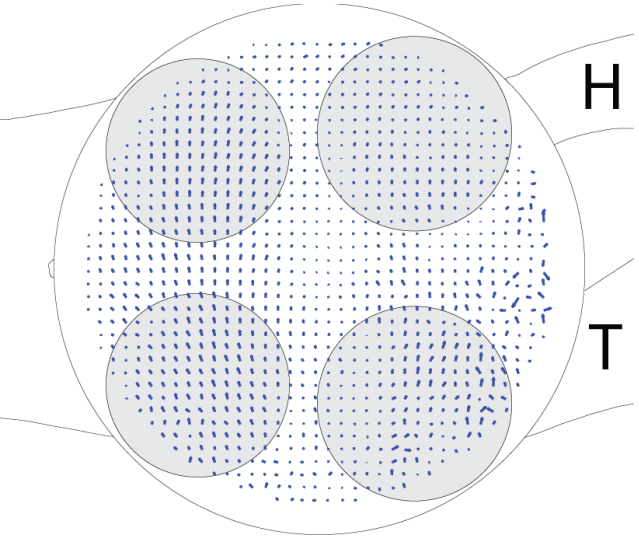

Rs,steady=2.2

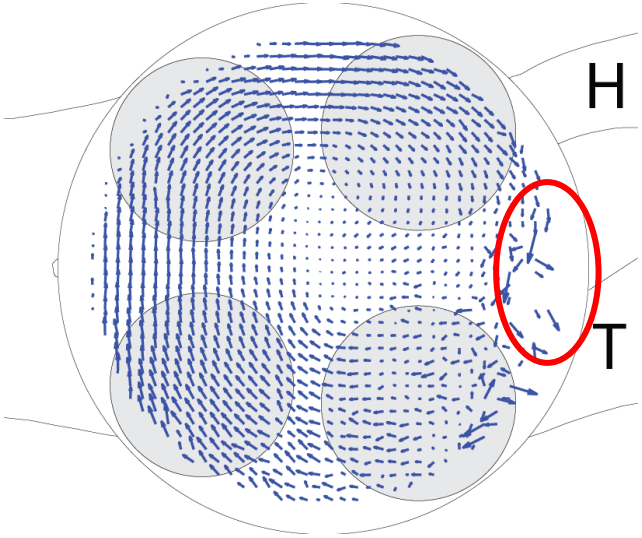

Rs,steady=3.5

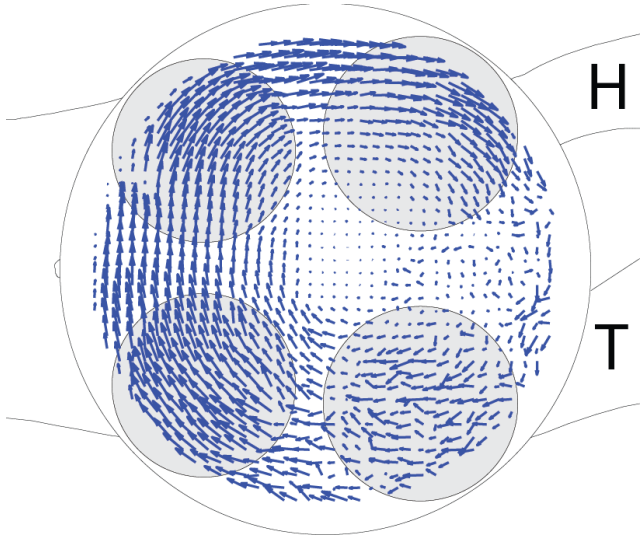

Ensemble mean-velocity over 100 cycles

-105ºaTDC

→ 5 S_p

GM swirl ratio index, z=10mm

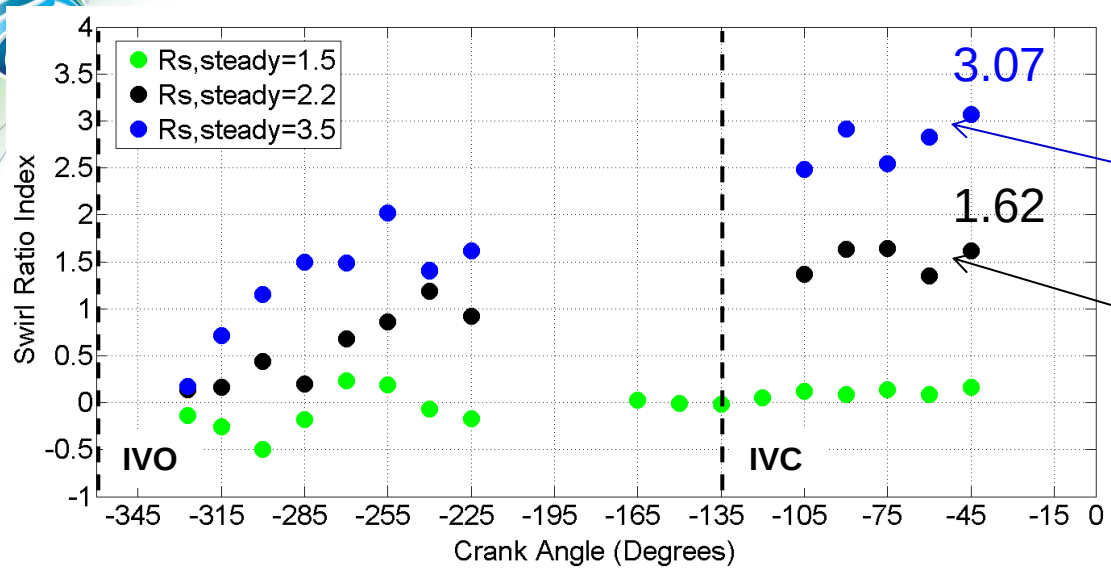

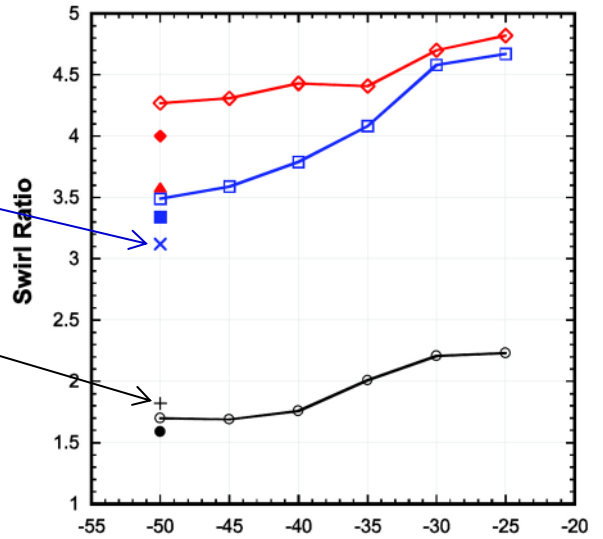

Petersen, SAE2011-01-1285

Rs,steady=1.5

Rs,steady=2.2

Rs,steady=3.5

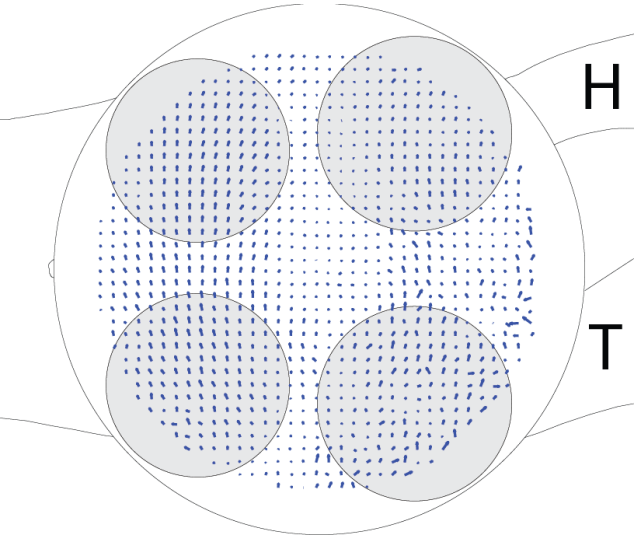

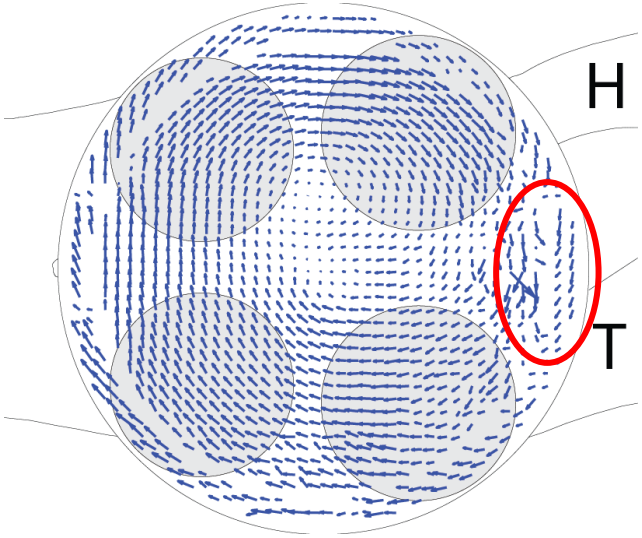

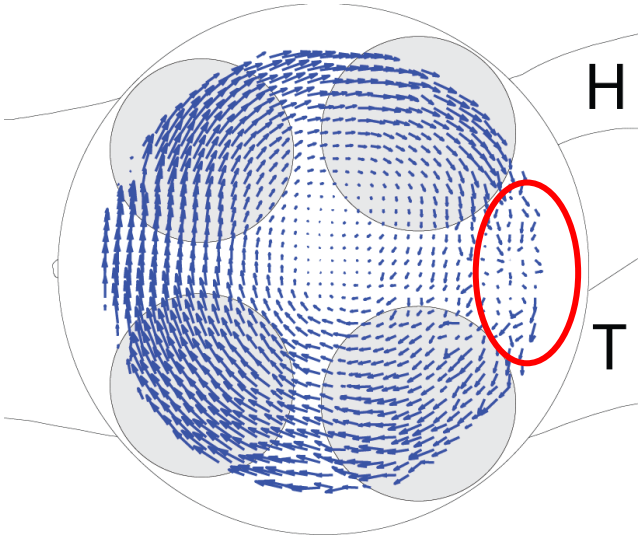

Ensemble mean-velocity over 100 cycles

-090°aTDC

→ 5 S_p

GM swirl ratio index, z=10mm

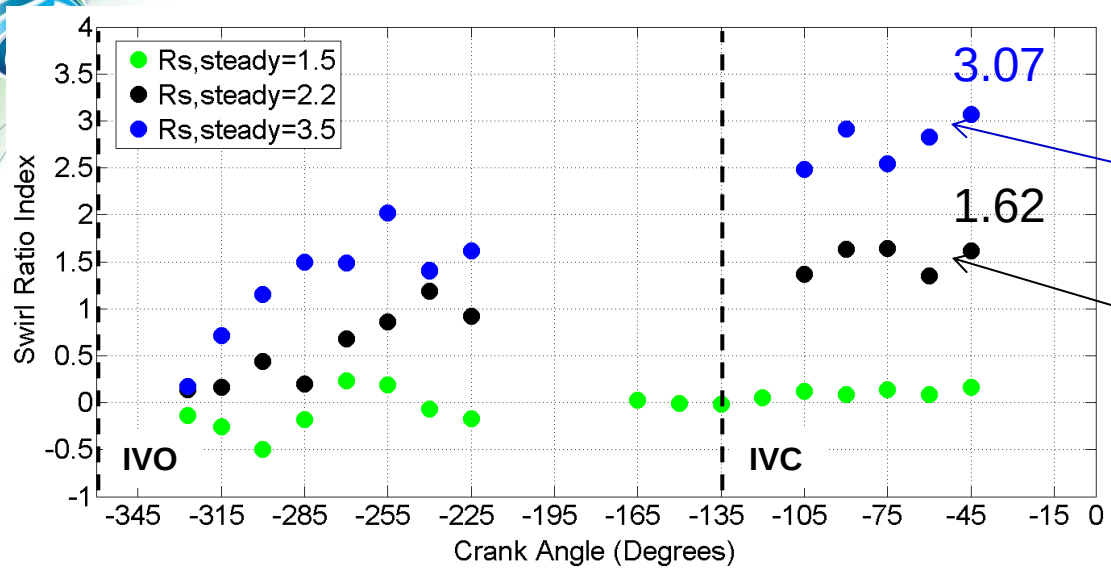

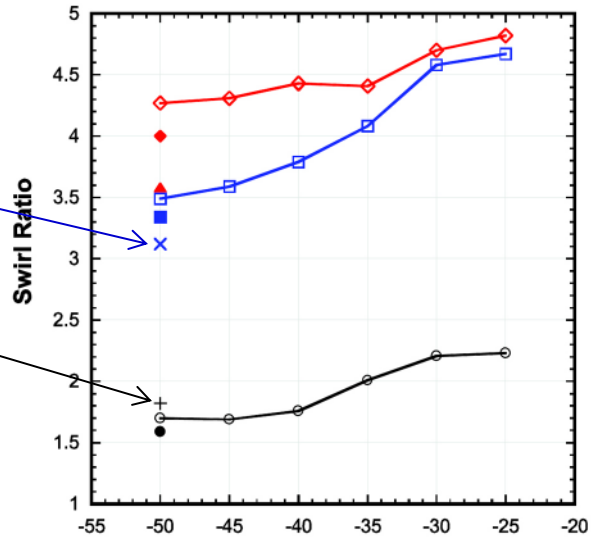

Petersen, SAE2011-01-1285

Rs,steady=1.5

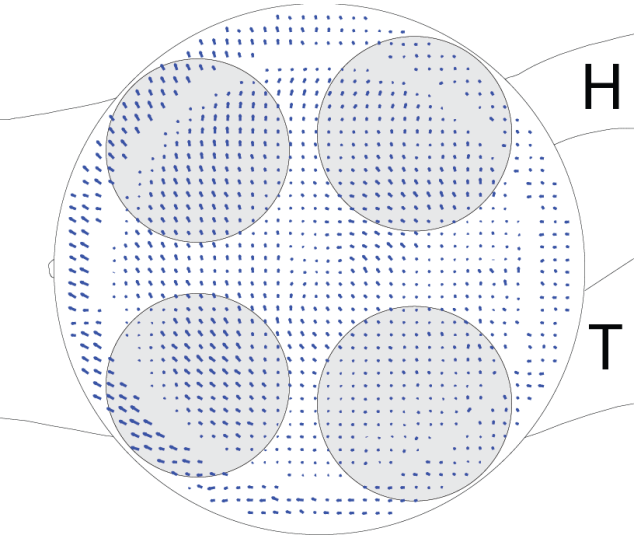

Rs,steady=2.2

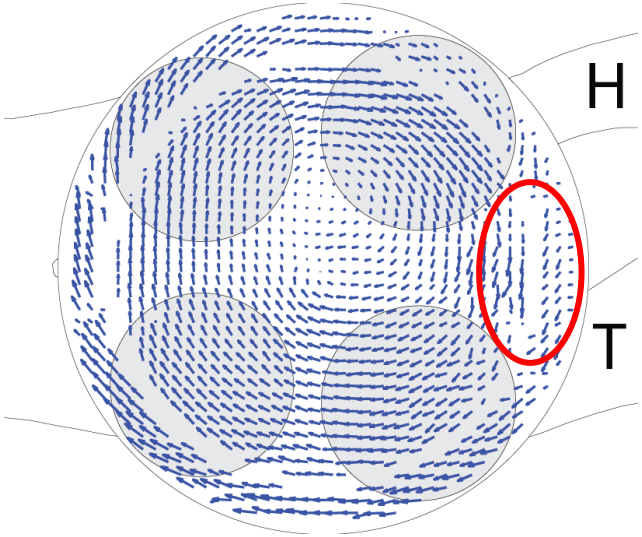

Rs,steady=3.5

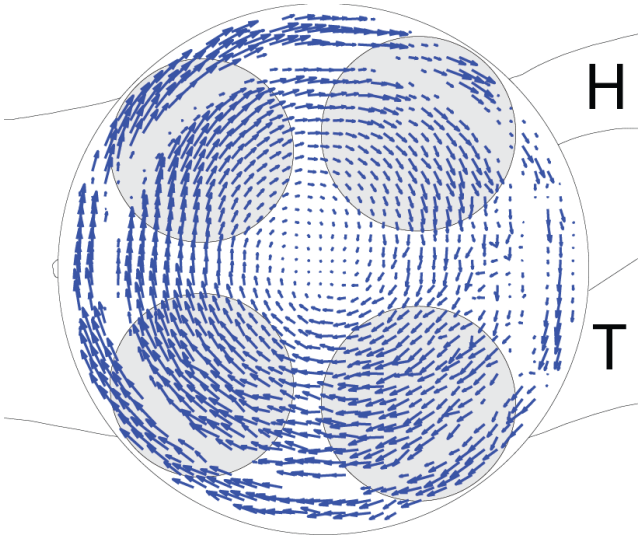

Ensemble mean-velocity over 100 cycles

-075°aTDC

→ 5 S_p

GM swirl ratio index, z=10mm

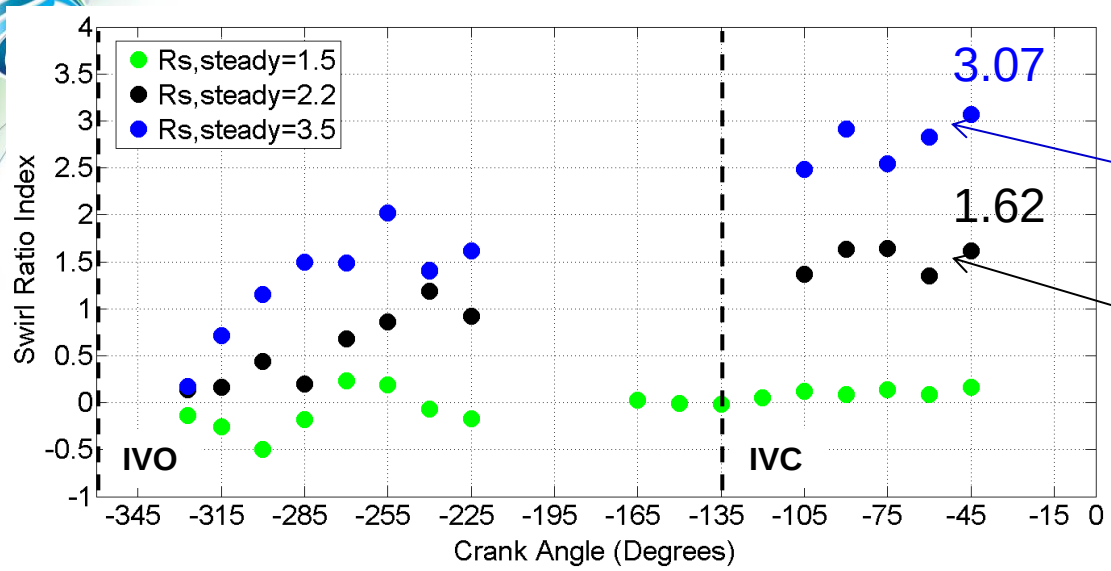

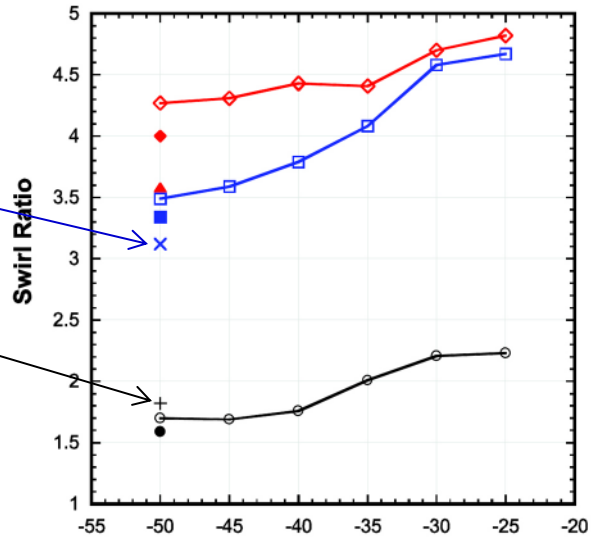

Petersen, SAE2011-01-1285

Rs,steady=1.5

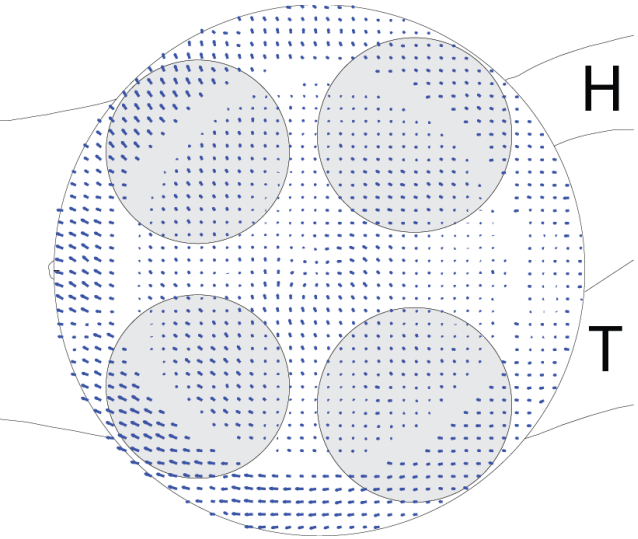

Rs,steady=2.2

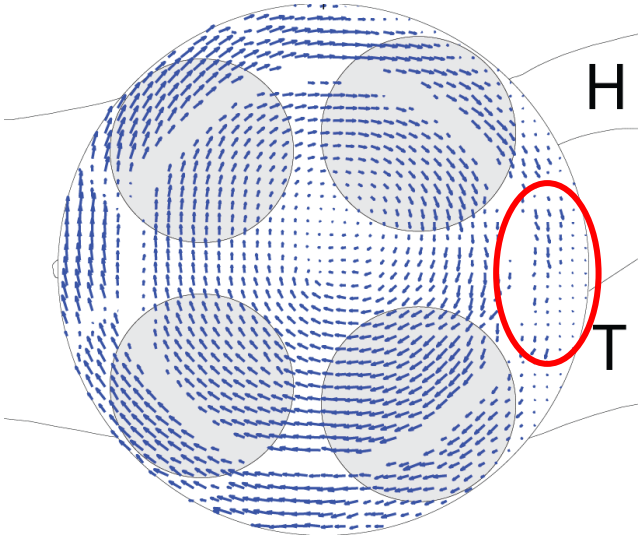

Rs,steady=3.5

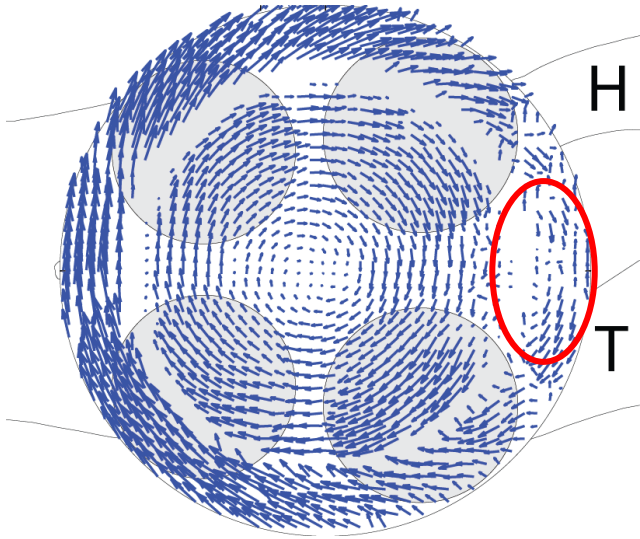

Ensemble mean-velocity over 100 cycles

-060°aTDC

→ 5 S_p

GM swirl ratio index, z=10mm

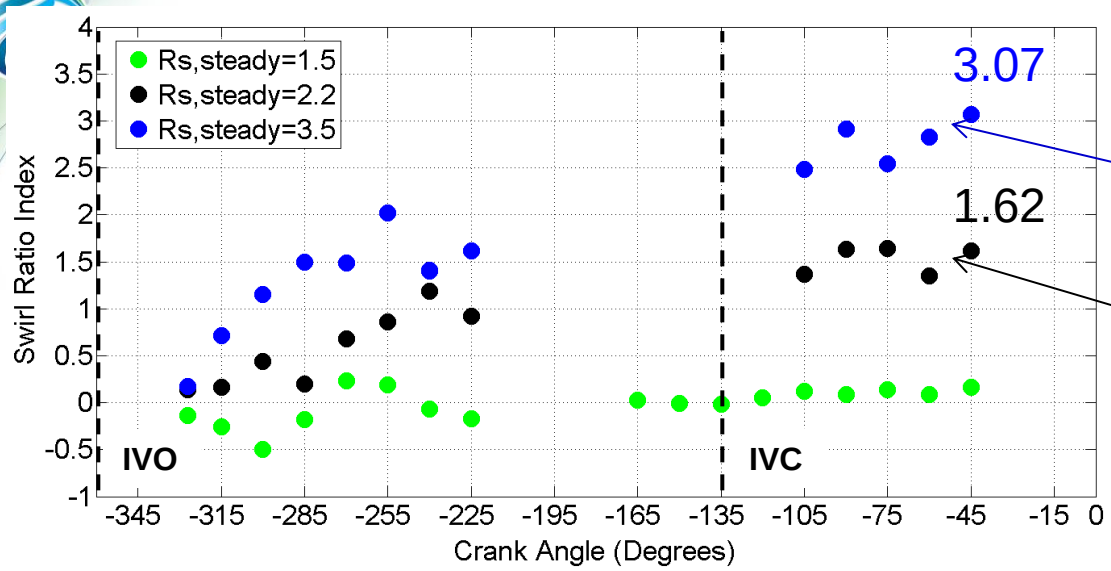

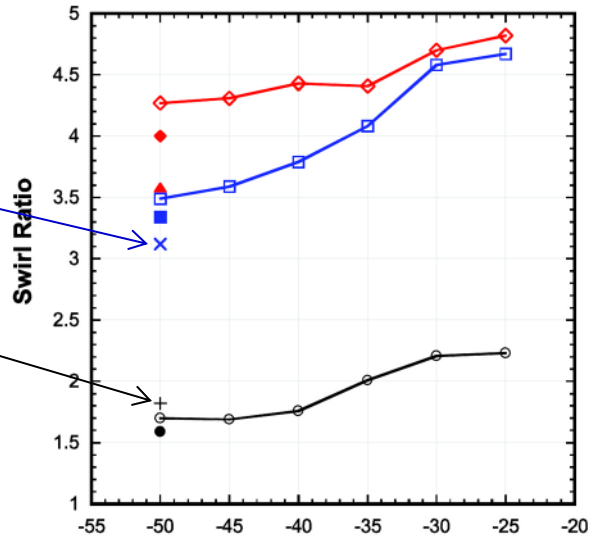

Petersen, SAE2011-01-1285

Rs,steady=1.5

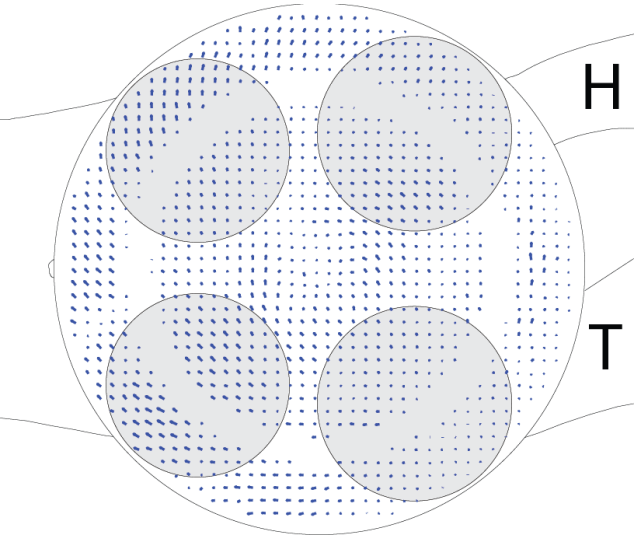

Rs,steady=2.2

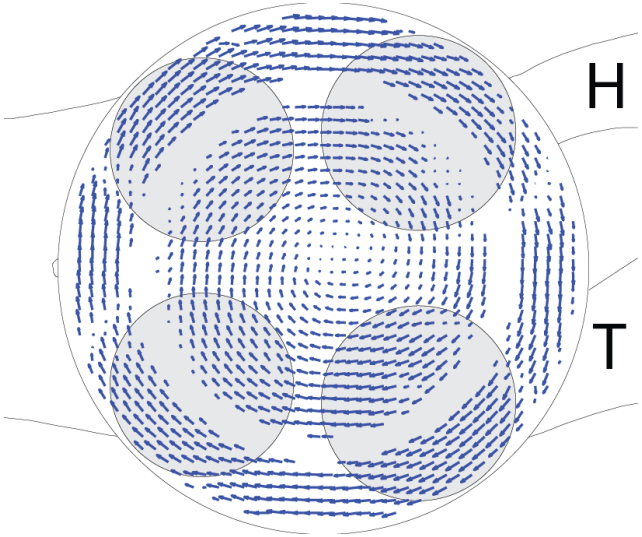

Rs,steady=3.5

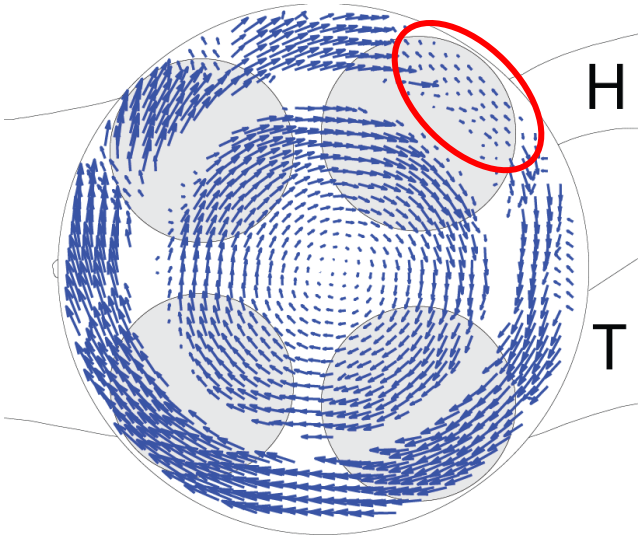

Ensemble mean-velocity over 100 cycles

-045ºaTDC

→ 5 S_p

Conclusions

- More detailed mean flow structures can be captured with 2μm borosilicate glass particles, but signal-to-noise ratio is too low late in the intake stroke and early in the compression stroke.
- Swirl ratio at -50ºaTDC is consistent with measurements done by Petersen SAE2011-01-1285 (18 μm borosilicate glass), the differences might come from the different definition of swirl centers.
- A few points need further attention:
  - Laser background scattering remains an issue with thick laser sheet.
  - Dewarping errors/artifacts will primarily result in velocity errors in the radial direction, but little impact on tangential velocities is expected.
  - The temporal interval between two laser pulses (Δt) must be optimized for particle displacement to match ~¼ of the interrogation window size at different crank angle position. (e.g. there exists a large dynamic range of velocity and out-of-plane motion during the intake stroke.)

Future work

- Improve Mie-scattering signal-to-noise ratio with thinner laser sheet and higher laser energy, 532 nm band pass filter on lens.
- Perform PIV in vertical planes (tumble plane and perpendicular to tumble plane).
- Investigate two different bowl geometries to study swirl centering and tilt.

$$\Gamma_1(P) = \frac{1}{S}\int_{M\in S} \frac{\left(\vec{r}\Lambda\overrightarrow{U_M}\right)\cdot\vec{z}}{\left\|\vec{r}\right\|\cdot\left\|\overrightarrow{U_M}\right\|} dS = \frac{1}{S}\int_S \sin\left(\theta_M\right) dS$$

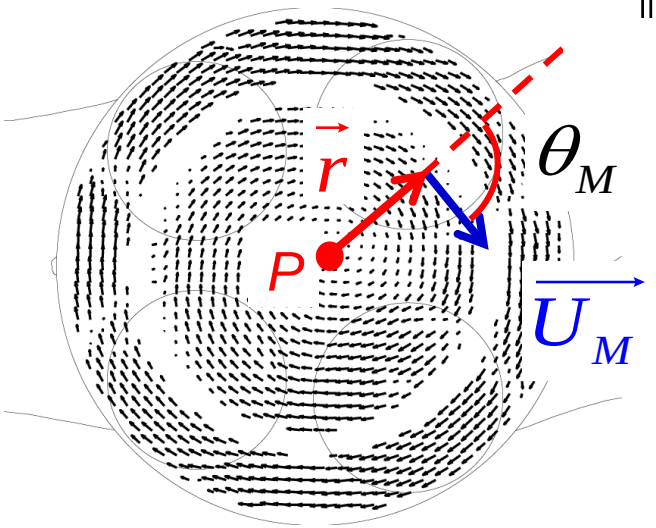

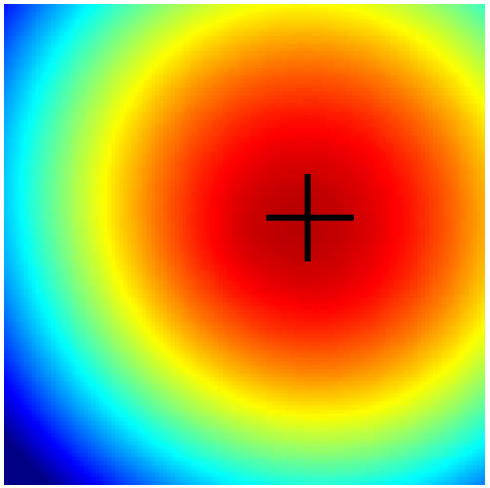

Graftieaux, L., et al. (2001). "Combining PIV, POD and vortex identification algorithms for the study of unsteady turbulent swirling flows." Measurement Science and Technology **12**(9): 1422-1429.

Backup Slides

To truly evaluate model results quantitatively, perhaps a simplified geometry is best?

Possible piston geometries:

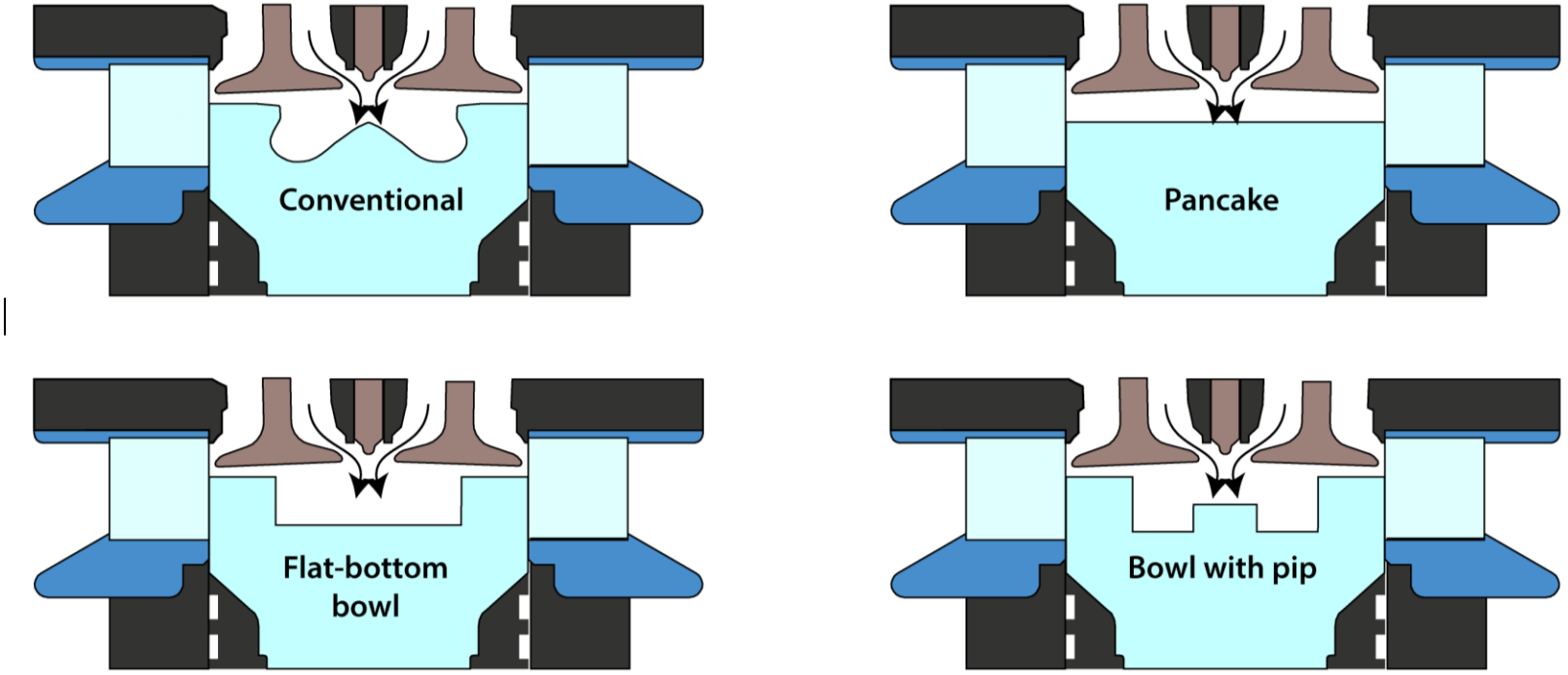

The data acquired would ***test the code***, they would not necessarily provide realistic engine flow structures

Is there any interest in these tests?